

Mainz, 13 October 2021

Dear Michel Van Roozendael,

we would like to submit a revised version of the manuscript AMT-2021-213 on “Calculating the vertical column density of O<sub>4</sub> from surface values of pressure, temperature and relative humidity” for consideration for final publication in AMT.

We have handled all issues raised by the reviewers and either modified the manuscript accordingly or provide detailed arguments in cases where we disagree.

Please find below

1. A general Corrigendum of three bugs made in the original manuscript:

(a) a mismatch in time dimension between O<sub>4</sub> VCDs based on GRUAN vs. interpolated ERA-Interim profiles.

(b) wrong number of available GRUAN profiles in Table E1 (now B1).

(c) consideration of all ECMWF pixels equally which causes an overrepresentation of polar regions.

These bugs were corrected in the revised manuscript. They did not affect the general results and conclusions of this study.

2. The detailed replies to all reviewer comments.

3. A tracked-changes version of the revised manuscript.

Note that this document overstates the changes actually made, in particular in the discussion (Section 5), where subsections were re-ordered, which was interpreted as complete deletion and new insertion by latexdiff. Thus we would like to also shortly list the main changes made in the revised manuscript:

- Section 2 has been revised slightly. The definition of effective lapse rate (previously given in Appendix A) is now given in section 2.3. The definition of the true O<sub>4</sub> VCD was shifted to section 2.4, as this is needed to understand how a and b are derived from a linear fit. The discussion of the modified parameterization of the O<sub>4</sub> VCD as function of RH<sub>0</sub> (section 2.5) was simplified, while the determination of a and b from a linear fit is now explained in more detail.

- Section 3 (Datasets) was shortened considerably by moving all details of minor importance for this study into Appendix B.

- Section 4.2 was largely revised and follows now a more straightforward logic by demonstrating that effective lapse rates are actually related to RH<sub>0</sub>. The linear fit of parameters a and b is now explicitly shown in a new figure.

- GRUAN results are now shown in a new figure (Fig. 8) instead of a table, including correlation coefficients as well as results from standard methods for the calculation of the O<sub>4</sub> VCD for comparison.

Section 5 was largely revised; sections 5.1, 5.2, and 5.3 from the AMTD paper became sections 5.6, 5.5, 5.4 in the revised manuscript. New sections discuss the comparison to existing methods (5.1), the impact of temperature inversions (5.2), and remaining impacts of humidity (5.3). The content of the former section 5.4 is now included in section 2.5, while former section 5.5 was added to Appendix A.

We hope that we have clarified all aspects raised during discussion phase and that the revised manuscript can be published on AMT.

Kind regards,

Steffen Beirle

## Corrigendum

We would like to thank both reviewers for the constructive feedback to our study, which helped to improve the paper. In particular, while preparing the replies to the reviewers, we noticed two bugs in the data presented in the AMTD paper:

1. As suggested by reviewer #1, we have checked the correlations of O4 VCDs based on GRUAN and interpolated ECMWF profiles. This comparison revealed that the time axis was flipped in the ECMWF data (while the intention was to flip the altitude axis only). I.e. the standard deviations for ECMWF listed in table 3 were too high, while the mean values were almost unaffected. We have corrected this in the revised manuscript. In addition, we now also correct for differences between surface altitudes from GRUAN vs. ECMWF, which has a large effect for mountain sites. The numbers for  $\delta_{\text{ECMWF}}$  have thus changed (generally improved) considerably.

2. As proposed by reviewer #2, we have added information on the time coverage of the analysed GRUAN sonde launches. By comparison with Table E1, we then noticed that the number of sonde launches did not match. Actually, Table E1 listed the number of *all* GRUAN profiles rather than just those for  $\text{SZA} < 85^\circ$ . We have corrected this in the revised manuscript.

In addition, we noticed a further necessary modification:

3. As the regular latitude-longitude grid of the global ECMWF data over-represents high latitudes, we now only consider the fraction of pixels corresponding to  $\cos(\text{lat})$  for each latitude for the calculation of histograms, means and standard deviations. This also affects the determination of fit parameters  $a$  and  $b$ , which have slightly changed. Consequently, all derived numbers that are based on  $a$  and  $b$  had to be updated accordingly. However, changes are in the permil range, and the general findings and conclusions of this study did not change.

## Reply to reviewer #1

We provide a point-by-point reply to the issues raised by reviewer 1 below. The original review is included in grey. Text changes in the manuscript are indicated in italic font.

Please also note the modifications made in the revised manuscript that are specified in the Corrigendum.

### 1. General comments

The manuscript "Calculating the vertical column density of O<sub>4</sub> from surface values of pressure, temperature and relative humidity" presents in varying level of detail the derivation of, and the validation of, a daytime applicable method to calculate the O<sub>4</sub> vertical column density from surface values of pressure, temperature and relative humidity. Hence, the title is well chosen. The main application area of this approximation are parametrized profile inversion algorithms for MAX-DOAS measurements. The authors also mention possible benefits for optimal estimation based profile inversion algorithms, stemming from the high correlation of surface relative humidity and temperature effective lapse rate. I recommend this manuscript for publication after intermediate revisions.

We thank the reviewer for the elaborated and thorough feedback to our study. We carefully considered the issues raised by the reviewer, and in many cases, they helped us to improve the paper. In some cases, however, we have a different point of view.

Below, we deal with the reviewer comments point by point. In cases where we disagree with the reviewer's evaluation, we motivate our point of view in this reply and in the revised manuscript.

While there is certainly scientific value in the presented method, the quality of the presentation and the structure of the manuscript, have to be improved. The validation of the method is not quite sufficient and has to be extended. The degree of explicit derivation of equations varies from "very detailed" to "almost insufficient" and should be brought to a more "equal" level.

We will refer to these aspects below when they are concretized by the reviewer.

The presented derivation of Eq. 9 seems unnecessarily complicated: Starting at the usual barometric formula for the air density for an atmosphere with constant lapse rate

$$\rho = \rho_0 \left( \frac{T_0}{T_0 + \Gamma(x-x_0)} \right)^{1+(gM/R/\Gamma)} = \rho_0 \left( 1 + \Gamma x'/T_0 \right)^{-(gM/R/\Gamma)}$$

( $x'=x-x_0$ ) and integrating the square of this  $\rho$  multiplied by the oxygen volume mixing ratio (i.e. integrate the O<sub>4</sub> density) from the surface (0) to infinity, replacing  $\rho_0$  by  $p_0/T_0/R$ , directly yields Eq. 9. Maybe the authors can comment on why they chose to over complicate things with introducing the ratio of  $h_{O_2}$  and  $h_{O_4}$ . (Likewise, choose the density formula for 0 lapse rate and integrate the square, in order to arrive at the corresponding equation for 0 lapse rate). I highly recommend to streamline this. I cannot see any added benefit of the method used by the authors, but I do see a lot of unnecessary turns given.

Equation 9 could indeed be derived directly, if a constant lapse rate is assumed. However, the concept of a constant lapse rate is a significant simplification, and real atmospheric profiles are more complex.

As pointed out in section 2.2, Eq. 6 is derived without any simplification or additional assumptions. Thus, the formalism derived in Equations 1 to 6 holds for any atmosphere, as we now state explicitly in the revised manuscript.

Equation 9 is a special case of Eq. 6 for constant lapse rate. For real atmospheric profiles, where lapse rate is usually not constant, still the formalism of Eq. 9 can be applied for the *effective* lapse rate, which was defined in Appendix A. This definition can only be understood in the context of equations 1 to 6. In the revised manuscript, we clarify this aspect by providing the definition of the effective lapse rate already in subsection 2.3.

At several occasions in the manuscript, the authors refer to later sections or to, at that point,

unproven and not referenced statements. This makes it impossible to read the manuscript in a linear fashion. The main line of reasoning should be clearly stated and followed.

(\*) We agree that reference to “future” sections is suboptimal, but we consider it sometimes unavoidable, as the line of arguments does not always follow a linear fashion. In addition, we think that it is not unusual to e.g. refer already in the result section to a specific aspect that will be discussed in more detail in the discussion section.

We decided to organize the manuscript having a section on formalism, followed by data sets and applications. Thus it is unavoidable that sometimes the motivation for choices made in the formalism is not directly supported by data. However, the alternative would be to jump forth and back several times between formalism, results, and discussions, which we do not consider as a better alternative.

In the revised manuscript, we have slightly revised the order of subsections in a more plausible order, and tried to minimize references to the “future” as far as possible.

Several statements are made without proof or proper reference.

We now support the respective statements with additional figures, concrete numbers or references.

Regarding style, the guidelines of AMT are, in several aspects, not followed.

We have adopted AMT guidelines in the revised manuscript.

The quality of the plots is mostly ok but should also be improved before final acceptance (especially the readability of axis labels).

We have revised the figures and increased the font size of axis labels.

Apart from the unfortunate structuring of the manuscript and the unnecessary turns given in order to arrive at the important equation, the biggest point of criticism is perhaps on the method validation and the lack of showing the improvement when using this new method over other methods to estimate the  $O_4$  VCD, as well as the actual effect on the final product, the retrieved AOD.

Three rather limited data sets were used for validation. Each of these datasets needs to be extended.

We are surprised by the evaluation of the reviewer. In the AMTD study, we have applied the derived formalism to  $\sim 1e7$  profiles from ECMWF,  $3e7$  from WRF simulations, and 6000 GRUAN sonde profiles. In the revised manuscript, we doubled the number of considered days from ECMWF by adding one day from autumn and spring, and we extended the application to WRF data to the full 2-month simulation period, increasing the number of WRF profiles to almost  $2e8$ .

Variability in space as well as fluctuations due to “weather” (high/low pressure systems) is well covered by the global ECMWF simulations. Variability in time is covered for several GRUAN stations. The derived statistical quantities are robust: standard errors of mean and SD are close to zero. From the different datasets, we derived quite consistent numbers for mean and SD. Thus, we consider the presented data to be sufficient for estimating realistic numbers for the errors made by the parameterisation.

For one of the datasets (global model), half of the dataset was used to fit parameters in the model; still, that same half was also used for validation. This should really be avoided. It is advisable to add a separate day for parameter fitting.

The calculation of  $\delta_{RH}$  for ECMWF data from 18 June is using the same data as used for fitting a and b. This is clearly stated in the manuscript. We do not consider this as validation, but rather as check of the fit performance (the SD of this comparison is related to the RMS of the linear fit).

We have now also processed ECMWF profiles for 18 March and 18 September, covering the full seasonal cycle. Results are very similar to those from 18 December. For the uncertainty estimates for ECMWF, we now explicitly provide the numbers for 18 March 2018, where highest deviations were found.

For the regional model dataset, the description seems to indicate that it consists of 2 months (May and June 2018, see line 179), although it appears that only a few days (beginning of May) were used to derive the statistics. It would be advisable to use at least 2 months covering different seasons (so instead of May and June, maybe June and December).

The WRF simulations were performed by Vinod Kumar for a different purpose. While the full model simulation was set up for a 2 month period, however, only 9 days of simulations were available at the time of preparing the initial manuscript. Meanwhile, WRF simulations for the full period are available, so we applied the formalism to the full period. Resulting frequency distributions for  $\delta_r$ , however, did only change slightly.

Running the WRF simulations at high spatial resolution is computationally expensive. As different seasons are covered by ECMWF data, we do not see the need for an additional WRF simulation for winter.

For the third data set, data from radio sounding, I believe there are plenty of data available since meteorological services such as the MetOffice, launch weather balloons twice a day at several stations (I believe the DWD does the same).

In this study we focus on sonde measurements from the GRUAN network, which provides high consistency and thus good comparability. Though the number of stations is limited, and some stations only contribute only few profiles, the GRUAN dataset still covers a wide range of conditions (latitude, climate, altitude).

In total, we have now applied the O4 calculation to more than 200 million profiles.

The derived statistics are robust; errors of the mean and SD are negligible, and results are similar for ECMWF, WRF and GRUAN sites for quite different conditions.

Thus we would argue that the conclusions drawn in this study are supported by the presented data, and additional radio soundings are not required.

In a next step, these results need to be compared to a "current standard method" approximating O4 VCD. This is entirely missing in this manuscript.

For MAPA, the "current standard method" of determining the O4 VCD is based on ECMWF data. This was already included in Table 3.

But we agree that the comparison to currently used methods should be extended. Thus, we

1. added the following sentence to the introduction:

*... modelled profiles might not be available in some cases (e.g. ~during measurement campaigns in remote regions and poor internet connection; for these cases, profiles from a climatology might be used as fallback option), ....*

2. added a new section (5.1) to the discussion, where the results for GRUAN profiles are compared to O4 columns from (a) daily model data, and (b) a climatology. In contrast to the discussion paper, we now correct for differences between surface altitudes from GRUAN vs. ECMWF, which has a large effect for mountain sites.

These comparisons indicate that the proposed calculation of the O4 VCD from surface values of p, T, and RH is indeed better than using profiles from a climatology.

I made a quick test using 3 years (2018, 2019 and 2020) of data from 6 stations (some overlap with stations that the authors use) from 12 UTC radiosonde launches (Cambourne [N=1061], Nottingham [N=315], Essen [N=468], Munich [N=1022], Lindenberg [N=1062], Lamont [N=430, 0 UTC for the latter to comply with the SZA requirement]). I find, using Eq. 12 and Eq. 13, respectively, a high correlation (0.93, 0.94, 0.92, 0.93, 0.93, 0.93) for estimated and integrated O4 columns (confirming the authors' findings), and, using Eq. 15, low bias and low standard deviation (-1.8±1.0)%, (-1.5±1.1)%, (-1.0±1.3)%, (-1.7±1.1)%, (-1.4±1.2)%, (-0.8±1.7)% (again, confirming the authors' findings). If I do the same but, instead of using the approximation method, use climatology data, I get the following for mean bias and std: (1.6±2.0)%, (0.1±2.1)%, (0.2±2.1)%, (-

3.9±1.7)%, (0.8±2.0)%, (-1.2±2.3)% (so 50 -- 100% worse standard deviation, but partly better mean). However, the correlations are certainly much lower (0.45, 0.51, 0.55, 0.65, 0.61, 0.53). I would like to see similar comparisons in the manuscript in order to show that using this method is in fact better than using climatology values [Is it actually worth it? Please show this!].

It would be advisable to include such statistics for at least 20--30 other well distributed weather balloon launching sites for a few years.

We acknowledge that the reviewer applied the formalism to additional datasets, and see the consistent results as confirmation of our argument that the number of profiles presented in this study is sufficient in order to support the drawn conclusions.

We have added comparisons to O4 VCDs (including correlation coefficients) based on a profile climatology in section 5.1, and could indeed show that both correlation coefficients and SD are worse for the climatology-based VCDs.

Lastly, since the use of this approximation is clearly, as the authors point out, tailored towards parametrized MAX-DOAS inversion methods, it is highly desirable that the authors show some result of those: compare the retrieval results using the "previously standard method" to results obtained using this new method.

The study was indeed motivated from a parametrized MAX-DOAS perspective. However, the manuscript has a clear focus on the calculation of the O4 VCD. We would like to keep this focus, and we do not see the need for adding MAX-DOAS inversions to this study, as the proposed parameterization of the O4 VCD can be directly compared to the "true" values based on vertical integration. Thus, we just provide a rough estimate of the impact of changes of the a-priori O4 VCD on AODs derived with MAPA for the CINDI-2 campaign.

The manuscript frequently refers to Wagner et al. 2019 which makes it appear to be rather suited as an extension of that publication than a stand-alone publication.

Wagner et al., 2019, is indeed cited frequently, as it also deals with the calculation of the O4 VCD. However, the current study has a clear focus of parameterizing the O4 VCD by surface values of p, T, and RH alone, without constructing vertical profiles. This, with the completely new mathematical formalism and the extensive validation, we consider it to be appropriate for a stand-alone publication.

From my point of view, the innovative part of this manuscript is the empirical relation between the effective lapse rate and the surface relative humidity and the fact that this knowledge can be used in the formalism of Wagner et. al 2019 to replace the fixed lapse rate. This part however, I do find sufficiently important for publishing.

However, the current format of the manuscript is not good enough. It over complicates things. It does not include sufficient validation data, nor does it include a test on the final product this method is thought to be used for. Hence, I recommend intermediate revisions of this manuscript.

Restructure the manuscript. Streamline and simplify the method section, especially how to arrive at Eq. 9. For validation, extend regional model data covering a larger time period, use a separate day for the parameter fitting for the global model, use many more datasets from radiosondes. Include comparisons with currently used methods (such as using climatologies). Include tests showing that the final product (AOD retrieved from MAX-DOAS measurements) in fact benefits from this new method to estimate O4 VCDs by comparing results ("old" and "new") to complementary measurements.

We have revised the manuscript in response to the comments of both reviewers. We have restructured the manuscript, but still stick to the separation into section 2 on formalism and section 4 on applications in order to avoid forth-and-back jumps between formalism, results, and discussion. Thus, references to the "future" have been reduced, but cannot be avoided completely. We have extended the application of the formalism to additional WRF and ECMWF data. In addition, we have added a comparison to O4 VCDs derived from a climatology.

As argued above, we keep the derivation of Equations 1-6, which hold generally for any atmosphere, and derive Eq. 9 (now Eq. 10) later as special case for constant lapse rate. The impact of a bias of the O4 VCD on MAX-DOAS profile retrievals is quantified in the introduction. We do not see the need for including additional MAX-DOAS profile inversions in this study, as the focus is set on the calculation of the O4 VCD.

## 2. Specific comments

- line 28: vertical profiles of T, P and RH are also needed to calculate the refraction index and hence are anyway needed for radiative transfer simulations, aren't they?

Within MAPA, the air mass factors used for the MAX-DOAS profile inversions are stored in a pre-calculated look up table based on RTM calculations using a standard atmosphere.

- line 33 -- 39: Here, the reader starts to wonder about the impact of temperature inversions. Later on (line 157), the authors mention temperature inversions and that they are far more frequent during night. Further, they mention that the main application is MAX-DOAS measurements and the presented method is limited to daytime. This should be already mentioned here, otherwise the reader will immediately wonder how temperature inversions are dealt with.

We added the following footnote to the introduction:

*Note that, for this approach, as well as for the parameterizations presented in this study, temperature inversions are problematic. As MAX-DOAS applications require daylight, however, night-time inversion layers are irrelevant for this study. The remaining temperature inversions at daytime, mostly occurring in early morning hours and over cold water and ice surfaces, will be discussed in Sect. 5.2.*

In addition, the impact of temperature inversions is now explicitly discussed in a new subsection 5.2 in the discussion.

- Section 2.1 seems largely unnecessary:

line 59 - 60: Incomplete list, and a 1 sentence paragraph: skip this.

line 61 -- 64: This should be skipped, does not add any new information (?)  $n_{\{O4,0\}} == n^2_{\{O2,0\}}$  is stated explicitly in Eq. 5

line 65 -- 68: No new information, all is contained in Table 1. Skip

We agree that Sect. 2.1 plus Table 1 adds some level of redundancy. However, we still consider it as helpful for the reader to also introduce the main quantities in the plain text. For instance, this allows to motivate the choice of units for O4 concentrations and column densities.

- Table 2: The  $g$  here corresponds to which latitude and which altitude? Since  $g$  varies about 0.5% between the poles and the equator, it should be important since the authors claim an accuracy of the same order of magnitude.

The value of  $g=9.80665 \text{ m/s}^2$  used in Metpy is the standard acceleration of gravity as listed in Tiesinga, Eite, Peter J. Mohr, David B. Newell, and Barry N. Taylor, 2020: The 2018 CODATA Recommended Values of the Fundamental Physical Constants (Web Version 8.1). Database developed by J. Baker, M. Douma, and S. Kotochigova. Available at <https://physics.nist.gov/cuu/Constants/index.html>, National Institute of Standards and Technology, Gaithersburg, MD 20899.

$g$  can be found on [https://physics.nist.gov/cgi-bin/cuu/Value?gn|search\\_for=acceleration](https://physics.nist.gov/cgi-bin/cuu/Value?gn|search_for=acceleration)

Actual gravitational acceleration at equator and poles differ from this value by less than 0.27%. This is one order of magnitude lower than the critical uncertainty of about 3%. Thus we consider the effects of latitudinal changes of  $g$  to be negligible. Note that also within ECMWF model data, the Earth is treated as sphere, using the same constant value of  $g$ :

<https://confluence.ecmwf.int/display/CKB/ERA5%3A+data+documentation>

In the revised manuscript, we added a footnote to  $g$  in Table 2 stating that the effect of latitudinal dependence is within 0.27% and thus negligible.

With the precision for C given in units of K Pa<sup>-2</sup> mol<sup>2</sup> m<sup>-5</sup>, the value for C in units of K hPa<sup>-2</sup> molecules<sup>2</sup> cm<sup>-5</sup> equates to 6.73267e39. The authors should consider to give one more digit of precision for the former units, so the unit conversion actually is consistent (a numeric value of 0.01856455 using the former units, which is consistent with the value given, indeed results [to the given precision] in the numeric value given using the latter units. However, as written now, it is not consistent). Is it really necessary to give the same constant in two different units?

In the revised manuscript, we provide only the second version of C, as this is the number needed in order to derive the O<sub>4</sub> VCD in the unit of molecules<sup>2</sup>/cm<sup>5</sup> which is usually used in DOAS context.

- As mentioned above, I recommend to rewrite everything up to Equation 9 and derive this equation directly from the integration of the density assuming either a constant lapse rate (Eq. 9) or 0 lapse rate (Eq.8).

As argued above, we consider the formalism of equations 1 to 6 as an important part of this study, as this holds for general profiles. In addition, the effective heights of O<sub>2</sub> and O<sub>4</sub> are needed in order to calculate effective lapse rates.

However, if the authors really want to stick to their complicated way of showing things (I highly discourage this!!), they should consider the following points:

line 88 -- 89: Neither of equations 7 or 8 is based on Eq. 6. Equation 7 follows, as the authors write themselves, directly from the equation of hydrostatic equilibrium and the assumption of a constant O<sub>2</sub> VMR (see comment below), Eq. 8 is simply the ideal gas law for quantities at the surface. Hence, this sentence should be moved to after line 100.

We do not claim that Eq. 7 or Eq. 8 is based on Eq. 6, but that the O<sub>4</sub> VCD can be related to surface pressure, surface temperature, and lapse rate. This first sentence summarizes the formalism derived in section 2.3 in plain words, and we think that it makes sense to start the section with this sentence.

Eq. 7: While the authors spoon feed the derivation of Eq. 6, they skip totally the derivation of Eq. 7 from the equation of hydrostatic equilibrium  $dp = -\rho g dz$ . (e.g. by  $P_{top} - P_{bottom} = -\rho g h$  - ( $P_{top}=0$ )-->  $-P_0 = -\rho g h$  --( $\rho = n \cdot m / vol$ )-->  $P_0/g = n m h / vol$  --( $n h / vol == V_{air}$ )-->  $P_0/g / m = V_{air}$ ). Apart from assuming that, it is also rightfully assumed that the volume mixing ratio is constant; although implicitly clear by Table 2, it should be added.

The surface pressure results from the total weight of the air mass above, which is directly proportional to the O<sub>2</sub> VCD. Thus, for Eq. 7, it is not necessary to integrate the hydrostatic equilibrium.

We have modified the paragraph to:

*Assuming a hydrostatic atmosphere, the surface pressure is just the gravitational force per area of the total air column.*

*Thus, the O<sub>2</sub> VCD is directly related to the surface pressure: ...*

We do not think that it is necessary to explicitly mention that the O<sub>2</sub> VMR is constant in the text, as it is listed in the table of constants.

line 98 -- 101 (+ Appendix A): All equations should have a number. Please add a number to the equation stated here. Also, reference the derivation of this directly as appendix A2.

The equations given in the text are just summing up the results of the derivation in Appendix A.

Giving them a number would result in having the same equation twice with different number.

In the revised manuscript, we clarify this by adding references to the respective equation numbers in Appendix A.

Regarding equation A3 from the appendix A2: Also here, a derivation of this equation is missing. Maybe start with the equation for polytropic atmosphere  $p/p_0 = (T/T_0)^{*(gM/R/\Gamma)}$  and  $T = T_0 + \Gamma * z'$  and say that Eq. A3 follows from this together with the ideal gas law.

We consider Eq. A3 as text book knowledge that does not need a derivation; for instance, it is provided on Wikipedia ([https://en.wikipedia.org/wiki/Barometric\\_formula](https://en.wikipedia.org/wiki/Barometric_formula))

I think there is something not going quite right with the signs: The authors define the lapse rate to be negative. As such (since  $g$  is defined positive in Table 2),  $-\alpha + 1 = -gM/R/\Gamma$  would be ( $\Gamma < 0$ ) a positive quantity. With this, the term in round brackets in Eq. A6 for  $z' = \infty$  would otherwise not disappear. I also wonder if there might be a minus sign missing in Eq. A6 in the last line (or  $z$  should be maybe going from 0 to  $-\infty$ , this solves the problems, I think, please check) ... We thank the reviewer for checking the formalism in such a detail and pointing out to an error in Eq. A6: indeed, the term in round brackets does not disappear for  $z' = \infty$ . However, this is not related to the signs, which we have checked to be correct.

We have investigated this in further detail and finally noticed, that a profile with a constant lapse rate cannot be extended to infinity, but has to end at an altitude of  $z_{TOA} = -T_0/\Gamma$ , which is about 46 km for  $T_0=300$  K and  $\Gamma = -6.5$  K/km. Above this altitude,  $T$  would be negative, and the number concentration given by equation A3 would be a complex number, which is both unphysical.

So the integration in equation A6 has to be performed from 0 to  $z_{TOA}$ .

In this case, the first term ( $z=z_{TOA}$ ) now vanishes, as the term in round brackets becomes 0, and the remaining equations A7-A9 are still correct.

We have modified this accordingly in the revised manuscript.

In line 429, what does "12" refer to? Eq. 12? It's easy to make mistakes, so it is of course also possible that I made a mistake in my checking. Please carefully check the signs anyway.

"12" refers to Eq. 12. The respective paragraph (now a new subsection in Appendix A) was revised accordingly.

- line 116 -- 128: The authors refer to a section "in the future". This is very bad practice. Reorganize the structure of the article in order to make it possible for the reader to follow. See general reply (\*) above (top of page 2).

- line 117 -- 118: Please explain this statement.

This section has been largely revised, and the statement has been skipped.

- line 118 -- 119: Please refer to the equation where you show that this statement is true. "effective" lapse rate is in fact not defined, what makes the lapse rate an "effective" one? In the revised manuscript, we define the effective lapse rate directly in subsection 2.3.

- line 127 -- 128: Please explain what you mean by this statement. Why "basically"?

We have largely extended the description of the fit of parameters  $a$  and  $b$  and reformulated and clarified this statement.

- line 130: The authors refer to "the future". Please restructure the manuscript.

We removed the reference to "the future" here as it is not necessary for the understanding of this section.

- line 163/ line 167: what does "truncation at T639"/ "truncation at T255" mean?

As explained in ECMWF FAQs, "the IFS model uses a spherical harmonic expansion of fields, truncated at a particular wave number. For example T1279 identifies truncation at wave number 1279. Each spectral truncation is related to a regular Gaussian grid, which is regular in longitude and almost regular in latitude."

<https://confluence.ecmwf.int/display/UDOC/What+is+the+connection+between+the+spectral+truncation+and+the+Gaussian+grids+-+Metview+FAQ>

In this manuscript, however, we do not want to go in such detail. We modified the text to “truncated at wavenumber 639/255”, and consider this information to be helpful for readers familiar with atmospheric models, while others could just read on.

- line 165: The authors are using one and the same day for fitting the parameters and for validation. This has to be changed.

We are aware that the 18 June cannot be used for independent evaluation of the parameterization performance, as the parameters were fitted for this day. This is also clearly stated in the manuscript. We now provide ECMWF uncertainties for a different day (18 March 2018) in the text.

- line 168: How is this a "pre-processed" data set if the authors use the model output and post-process it?

This processing was made by ECMWF, so from our perspective, it is a pre-processed data set.

- line 195: Are the authors following some recommendations with this? If so, please cite. Otherwise, please explain why this choice justifies the statement "only retain the measurements of the highest quality".

In order to avoid a too detailed description in the main manuscript, we have moved this section to the appendix. We have modified the respective paragraph as follows:

*Additionally we have applied quality control filters such that the parameters QUALITAETS\_BYTE (QB) is below 4 (thereby excluding untested, objected, and calculated values), and QUALITAETS\_NIVEAU (QN) is either 3 (automatic control and correction) or 7 (second control done, before correction) to only retain measurements of high quality; note that using only data with QN=10, as recommended in the DWD description, would result in having almost no data left. Additionally, we have applied quality control filters such that the parameters QUALITAETS\_BYTE (QB) is below 4 (thereby excluding untested, objected, and calculated values), and QUALITAETS\_NIVEAU (QN) is either 3 (automatic control and correction) or 7 (second control done, before correction) to only retain measurements of high quality. By applying these criteria, we retained 98.2%, 100%, and 99.5% of T0, p0, and RH0 data, respectively. Note that using only data with QN=10 (the best possible quality check level) would result in no data left for the period considered in this study. If only QN=7 had been applied, we would have retained the same number of T0 and RH0 but no p0 data.*

- Fig. 1: Can the authors comment on the apparent differences between the models and the GRUAN measurements about the covered parameter space? The author mention the very high values, but do not comment on the many missing intermediate values.

We have modified the figure caption as follows:

Low values correspond to high altitude sites with low surface pressure; for GRUAN, only few of such stations are available (Boulder and La Reunion at 1.7 km and 2.2 km altitude, respectively).

The authors use 2 months of WRF data but choose to show only a single day (in a). The authors say that this is in order to keep the figure readable. I suggest to include a second row showing all the data. From statements elsewhere in the manuscript, I have the impression that even the data used for the statistics is not the full 2 months, but only a few days from the beginning of May. Is this correct, if so, why?

- line 217 - 218: Please show this in a plot (see comment above, include all data points).

In the revised manuscript, we now present 2d histograms instead of scatterplots, and include the complete 2-month WRF data set.

- Sect. 3.2: The little detail given is really not well structured. I suggest to include a thorough description as an appendix.

As proposed by the reviewer, we have moved this paragraph to the appendix, and slightly modified its structure.

- line 219 -- 220: This statement is not quite correct. In terms of covered V, both WRF and GRUAN cover roughly  $\hat{\tau}V = 0.7e43 \text{ molec}^2/\text{cm}^5$ , where WRF covers the space more evenly, GRUAN has a gap of  $\hat{\tau}V = 0.2e43 \text{ molec}^2/\text{cm}^5$ .

The statement was not referring to the variability of the O4 VCD, but to the variability of slopes (corresponding to different lapse rates). We have modified this sentence to *ECMWF and GRUAN data show higher variability in slopes ...*

- line 225: Where do you show that this statement is correct? There is no direct comparison made. Either include such a comparison or remove this statement.
- line 229: Please show this 0.5% explicitly.

In the manuscript draft, we have discussed and quantified the difference between Eq. 9 and the approach proposed in Wagner et al. in Appendix A2 (lines 425-429).

In the revised manuscript, we extended this discussion in a new subsection of (Appendix A3) and explicitly calculate the effect of neglecting the tropopause on the O4 VCD.

- Figure 2: Why is the histogram only considering 8 days instead of the complete 2 month data set? Or do I understand this incorrectly?

In the revised manuscript, results from the full 2-month period are included in the WRF histograms. The resulting frequency distributions of  $\delta_T$  and  $\delta_{RH}$ , however, changed only slightly.

- Figure 3: Maybe comment on great lakes in North America in summer.

We would like to thank the reviewer for pointing this out. We had a closer look at the profiles above the Great lakes and noticed a strong near-surface temperature inversion due to the cold water. Similar effects are visible over the oceans where SST is low.

We have added the following sentence to the manuscript (at line 237, after “High values ... over ocean.”):

*In particular over cold water surfaces, like the West coast of North and South America, the Hudson Bay, or the Great lakes,  $\delta_T$  is very high (up to 7%). This is related to temperature inversions close to ground: due to the too low surface temperatures, the O4 VCD calculated from Eq. 10 is biased high.*

In addition, we have added a new Figure (Fig. 9) showing maps of temperature gradients close to the ground, and discuss the impact of temperature inversions in a new subsection (5.2) in the discussions.

- line 238 - 239: You do not show this. Either show it (appendix?) or remove this comment. We removed this comment.

- line 239 - 240: Can you prove this statement? Please show a plot of lapse rate vs.  $\delta_T$

In the revised manuscript, we have added a new figure, showing maps of the effective lapse rate for ECMWF data on 18 June 2018, supporting our statement.

- line 242: How is this considered (implicitly due to known profiles)?

We have specified the description about how the true O4 VCD is derived as follows:

*... we also calculate the “true” O4 VCD, which is derived by*

*(a) calculating the profile of  $n_{O2}$  from profiles of  $T$ ,  $p$  and  $RH$ . In this step, the effect of humidity is explicitly accounted for by subtracting the water vapor pressure before calculating  $n_{O2}$  based on the ideal gas law. ...*

Also include a reference and an equation using the partial pressures of dry air and water vapour which makes the dependence on specific humidity apparent.

- line 243: Please define specific humidity (mass ratio of water vapour content and total mass of air parcel) and relate it to relative humidity (ratio of water vapour pressure and equilibrium water vapour pressure).

We have modified the line of arguments concerning humidity effects. We directly introduce and motivate the parameterization of effective lapse rate and thus the O4 VCD based on RH<sub>0</sub> in Sect. 2.

The effects of humidity on O4 number density are also (at least partly) covered by the empirical fit of a and b, and the impact of specific humidity turned out to be not critical for the proposed parameterization, as we now demonstrate in a new subsection in the discussions, where we directly check the relation between  $\delta_{RH}$  vs. specific humidity and TCWV.

Since no significant effects were found, we would like to keep this discussion on a more general level, and we would prefer not to add additional formulae which are irrelevant for this study.

- Sect. 4.2.: The authors lack to clearly state the logical chain of causes here: relative humidity affects effective lapse rate. Lapse rate affects V.

We have strengthened the logical chain accordingly.

- line 250 - 256: Make a plot as Fig. 3 using effective lapse rate calculated from the ECMWF model to show that this statement is correct.

In the revised manuscript, we have added a new figure, showing maps of the effective lapse rate for ECMWF data on 18 June 2018. In addition, we provide 2d histograms of effective lapse rate versus RH<sub>0</sub>.

- Sect. 4.3.:

It is stated that ECMWF data from June, 18th 2018 was used for the fit. Further, the authors state (line 267) that they investigate June, 18th 2018. This should never be done. You cannot use the same day for fitting and verification. Please choose a third day for the fitting and use the same day (June 18 and December 18) only for verification.

We are aware that the 18 June cannot be used for independent evaluation of the parameterization performance, as the parameters were fitted for this day. This is also clearly stated in the manuscript. In the revised manuscript, we provide results for 18 March for evaluating accuracy and precision.

- line 264: Please state clearly which figures to compare. Also, it seems that for certain regions (e.g. the Andes, central Europe around lunch time), the absolute value of  $\delta_{\Gamma}$  increased. It might make sense to show a map of the relative improvements of  $\delta_{\Gamma}$ . (? or maybe not...)

We added references to the figures showing  $\delta_{\Gamma}$  and  $\delta_{RH}$  for WRF and ECMWF. There are actually few regions where  $\delta_{\Gamma}$  is closer to 0 than  $\delta_{RH}$ , but this is no contradiction to the frequency distributions of  $\delta_{\Gamma}$  and  $\delta_{RH}$ .

Relative improvements would require divisions by small numbers, as  $\delta_{\Gamma}$  and  $\delta_{RH}$  are close to 0. This would lead to instabilities.

- Table 3: Include, in analogy to Eq. 14 and 15, an equation for  $\delta_{ECMWF}$ . Include also a histogram for the data in Table 3 in analogy to the histograms in Figs. 2,3,4,6,7,8. Why do the authors not present a correlation plot of V true and V parametrized? I think this is could be very instructive (I made it for the aforementioned stations and it looks very nice).

Instead of including a further definition for  $\delta_{ECMWF}$ , we now just define the deviation in a generic way for  $\delta_x$ , where x can stand for  $\Gamma$ , RH, or ECMWF.

We do not present GRUAN results in form of a histogram, as the separation for different stations would be lost. Instead, we now present GRUAN results in a new figure (Fig. 8) which also includes the comparison to O4 VCDs based on daily as well as climatological ECMWF profiles. We also

included the respective correlation coefficients to this figure. We don't consider additional scatterplots necessary here.

- line 301: with "radiation shield", you mean a Stevenson screen?

Direct solar radiation must be shielded from the thermometer, otherwise the measurements cannot be used. Stevenson screens are used for stationary meteorological stations. But there are also small, portable devices available with integrated radiation shields, which might be easily installed next to a MAX-DOAS instrument. So we keep the sentence as is.

- line 303: What is sufficient?

As stated in the introduction, the uncertainty of the O<sub>4</sub> VCD should be below 3%. In order to make this more clear, we extended the respective sentence in the introduction to

*Thus, for MAX-DOAS profile inversions, the O<sub>4</sub> VCD should be determined with accuracy and precision better than about 3%, which limits the impact on resulting AODs to below 10% and leaves other sources of uncertainty, i.e. the spectral analysis ( $\approx 5\%$ ) as well as radiative transfer modeling ( $\approx 4\%$ ) (see Wagner et al., 2021, Table 3 therein) as the limiting factors.*

- line 319 - 320: Please explain what you mean by "and V<sub>O<sub>4</sub></sub>, RH is almost the same for WRF and ground stations".

We meant that the diurnal cycles of V<sub>O<sub>4</sub></sub>, RH is almost the same for surface data from WRF vs. DWD. This statement is not as clear for the revised results based on 2 months of WRF simulations. We have revised the paragraph accordingly.

- line 334: What is sufficiently here? Why do you judge it to be sufficiently?

We have modified this statement to

*Thus, the parameterization of eq. 14 also reflects most of the diurnal cycle of the O<sub>4</sub> VCD, with remaining systematic errors below 0.3%.*

- Figure 10: How did you choose the points to be plotted? Are the correlation values indicated still using all points?

For the calculation of correlation coefficients, all data points were used. The scatter plots showed a subset by just selecting pixels in steps of 100 in order to keep them readable.

In the revised manuscript, we replaced all scatterplots by color-coded 2d histograms based on the complete data set.

- line 354: Where does the 3% estimate come from?

In the revised manuscript, we provide concrete numbers for  $\delta_{RH}$  for elevated sites, which are actually lower than 3% after skipping profiles affected by temperature inversions.

- Sect. 5.5: How do you measure S<sub>O<sub>2</sub></sub>?

In response to the comments of reviewer 2, we have moved this section into the Appendix (App. A4). In the revised manuscript, we modified this section and now only refer to the VCDs of O<sub>2</sub> and O<sub>4</sub>.

- line 379: Why "basically"?

We have removed "basically".

- line 386: Why is it sufficient?

We have extended this sentence to

*This accuracy and precision of  $< 3\%$  is typically lower than other uncertainties of spectral analysis or radiative transfer modelling (Wagner et al., 2019).*

- line 389: Inside a Stevenson screen I assume, otherwise the readings might be rather useless. See reply to line 301 above. We modified the sentence to ... *state-of-the-art thermometer (with radiation shield), barometer, and hygrometer.*

### 3. Technical comments

#### 3.1 general

Since one of the co-authors is the chief-executive editor of AMT and the first author is an associate editor, I find it slightly worrying that the authors disregard so many of the AMT guidelines:

**We thank the reviewer for listing the inconsistencies to AMT guidelines. In the revised manuscript, we have resolved most of the raised issues. In addition, Copernicus office will take care of consistent style and format during the copyediting process.**

- The journal guidelines clearly state that the recommendations of the SI brochure and the IUPAC Green Book (links can be found here: <https://www.atmospheric-measurement-techniques.net/submission.html#math>) should be followed. This is largely neglected in the axis labels and table headers. Physical quantities and units should not be written as "quantity [unit]" but as "quantity/ unit". Consider SI brochure Sect. 5.4 or alternatively, page 3 of the IUPAC Green Book. Please adjust this throughout the manuscript.

**As noted by the reviewer, this is a recommendation, but not a strict standard. Thus we prefer to provide units in brackets in figure axis, which is also commonly done in most of recently published AMT papers.**

- The journal guidelines clearly state that universal time should be indicated as "UTC". Please correct all "utc" (e.g. Figure 9) in the manuscript.

**Done.**

- The journal guidelines clearly state (<https://www.atmospheric-measurement-techniques.net/submission.html#figurestables>) that table should be written Table if followed by a number, please correct throughout the manuscript (e.g. line 26, 263, 283, 306).

**Done.**

- The journal guidelines state: "Coordinates need a degree sign and a space when naming the direction (e.g. 30° N, 25° E)". This is not done anywhere, please correct throughout the manuscript (e.g. in Fig. 2, 6, B1 and C1, in Table E1, line 175 no space is included).

**Done.**

- Inconsistent use of section (most of the manuscript) vs sect. (line 279, 217). Journal guidelines say "Sect." unless at the start of the sentence. Please correct.

**Done.**

- Inconsistent use of fig. (e.g. line 177, 197), Fig. (e.g. 216) and Figure (338). Journal guidelines say "Fig." unless at the start of the sentence. Please correct.

**Done.**

- Inconsistent use of equation (e.g. line 360) and eq. (Table 2, line 83, 88,...) Journal guidelines say "Eq." unless at the start of the sentence. Please correct.

**Done.**

- The journal guidelines clearly state not to use hyphens for ranges, but to use en dashes to indicate ranges (<https://www.atmospheric-measurement-techniques.net/submission.html#english>). However, the authors use sometimes hyphens (e.g. Fig.9 caption). Other times they use "to" which,

according to <https://www.atmospheric-measurement-techniques.net/submission.html#math> is ok. Please change the hyphens to en dashes or "to".

We use “to” for indicating ranges in the revised manuscript.

- "data" should be considered plural (<https://www.atmospheric-measurement-techniques.net/submission.html#english>). Please correct throughout the manuscript. (e.g. 253, 169, 460)

Done.

3.2 specific

- line 14: What is absorbed is the light, not the O<sub>4</sub>, hence "O<sub>4</sub> absorption in scattered light" is not a correct formulation. (Maybe add "pattern"?)

We have added “pattern”.

- line 15: "light path distributions in the atmosphere" seems also not quite correct.

We do not see a problem here.

- line 15: "light path increases" should be "light path length increases"

Done

- line 16: "cloud heights": be more specific: cloud top heights or cloud base heights?

As the O<sub>4</sub> signal is caused by a complex combination of light path shortening or lengthening and multiple scattering inside the cloud, it is neither top nor bottom, but rather something in between.

As this is not the focus of this study, and a more specific statement would require additional explanations distracting from the main line, we would prefer to keep this statement unspecific here.

- line 29: "[...] measured profiles [...] do not provide continuous temporal coverage [...]" The profiles do not provide temporal coverage of what? (of itself?) This a somewhat awkward formulation, please reformulate

We changed the subject to “radiosonde measurements”.

- Table 1: "Relative deviation between of parametrized and true O<sub>4</sub> VCD" --> remove "of"

Done.

- Table 2: replace e+39 by " $\times 10^{39}$ "

Done.

- line 70 -- 82: Why so wordy? Eq. (1) -- (3) can be summarized in one line of equation without the unnecessary text.

We consider it necessary to introduce equations 1 to 3 with some level of detail, even if the single steps seem trivial. In particular for the definition of the effective lapse rate, the concept of the effective height is required.

- line 86: add coma: "So far, .."

Done.

- line 117: "on first glance" --> "at first glance"

Done.

- Eq. 12: inconsistent accuracy of C (c.f. Table 3).

In Table 3, constants are now provided with high and consistent accuracy. For the final equation given in the plain text, which should be applied by the user, less digits are sufficient, given the remaining uncertainties.

- line 156: add "profiles" after "daytime".

Done.

- line 159: "selecting data for ..." wrong preposition.

We replaced the preposition by "with".

- line 164: add a coma after "here"

Done.

- line 177: Insert coma after "Vertically"

Done.

- line 180: Reverse the sentence. Start with "For constraining.... we use..." otherwise it is confusing why you start again with ERA5 data.

Done.

- line 180: include "of" after resolution

Done.

- line 184: "The selection of  $SZA < 85^\circ$ " is not correct. You do not select the SZA, you select data at times of the day at which  $SZA < 85^\circ$ . Please reformulate.

We modified this sentence to

*The selection of data with  $SZA < 85^\circ$  ...*

- line 185: replace "reach up to a pressure level" by "extend to a pressure of" or similar.

Done.

- line 211: "if" --> "of"?

Corrected.

- line 212: Please reformulate this sentence (especially "apply eq. 9 in section...")

We have reformulated this sentence.

- Sect. 4.1. title: add "a" before function.

Done.

- Fig. 1: axis labels are too small. Figures are too small, extend to page width. Legend box partly covers line. "mountaineous" --> "mountainous" or better: high altitude. If the authors choose to use only y-tick labels and y labels on the first subplot, the hspace should be 0.

We have increased font size for axis labels. The figure width was on purpose chosen as  $\frac{3}{4}$  of page width, in order to have the same subpanel size for figures 1, 5, 10, and D1 (now: 1, 5, 10, 11, B3). The legend box was adjusted. We modified the caption to "high altitude". y-tick labels are now shown for all subplots.

- line 218: add "the" in front of "highest"

Done.

- line 219: "matching to a lapse rate" needs reformulation

We have replaced “matching” by “in accordance”.

- line 230: The choice of  $\delta_{\Gamma}$  is not the best, it seems to indicate that the  $\delta$  is w.r.t  $\Gamma$  while it is w.r.t.  $V$ . Please consider renaming. Is it really "parametrized" yet? As I understand, the authors apply Eq. 9 with the constant lapse rate. So I do not see any parametrization here.

$\delta$  is used as symbol for relative deviations between calculated and “true” O4 VCDs. So both  $\delta_{\Gamma}$  and  $\delta_{RH}$  refer to differences in  $V$ . But we tried to discriminate the results for the two investigated approaches by a clear, but short subscript. We think that “ $\Gamma$ ” (using the lapse rate as parameter, thus “parametrized”) and “RH” (using RH at ground as parameter) fulfil this purpose.

- Figure 2: Please repeat the meaning of  $\sigma$  and  $\mu$  (from line 147) in the figure caption. Swap color bar and histogram, include ticks on the right hand side of the histogram. Please consider putting the coordinates at the axis instead of in the middle of the figure (same for Fig. 4).

We do not use  $\sigma$  and  $\mu$  any more in the revised manuscript. We would like to keep the arrangement of the subpanels as is in order to have the color bar next to the maps it refers to. Putting the lat/lon coordinates at the axis would need additional space outside the maps, and consequently further shrink down the maps in the subpanels. Thus we would prefer to have the lat/lon coordinates inside the figure.

- line 235: "Also for ECMWF data..." should really be something like "Considering ECMWF data as the basis for calculating  $\delta_{\Gamma}$ , also results in  $\delta_{\Gamma}$  values close to 0 for the area covering Germany". Please reformulate.

We have modified this sentence to

*For ECMWF data on 18 June 2018,  $\delta_{\Gamma}$  over Germany is close to 0 as well.*

- line 237: "For continents..." needs reformulation.

We have modified this sentence to

*Over continents,  $\delta_{\Gamma}$  is lower, and generally close to 0, except over deserts, where negative values are observed.*

- line 238: It is advisable to stick to either abbreviations or the symbolic notation, do not mix.

We use the terms mean and SD throughout the revised manuscript, and skip  $\mu$  and  $\sigma$ .

- line 239: insert "the" in front of "same".

Done.

- Figure 3: Add year after "18 June" (or reformulate to "the same day").

Done.

- Figure 4: Add year after "18 December" (or reformulate, see above).

Done.

- line 242: I think it is more correct to refer to the density instead of the weight of air. Please reformulate.

We now state that addition of humidity reduces the O2 number density.

- line 244: Is "compared" really the correct verb to use here?

As we show both quantities in a scatterplot (now 2d histogram), we think that we “compared” the quantities.

- line 252: "Subsidence" of what?

We have extended the discussion of the relation of RHO and effective lapse rate in section 2.5, including the effect of “large-scale subsidence of air masses”. The text in line 252 has been skipped.

- line 257 -- 259: Please reformulate and clearly state that you used Eq. 11 to fit parameters a and b and the result is Eq. 12. As it currently reads, it is hardly comprehensible.

We have largely revised and extended the description of how the linear fit is performed to gain a and b, including a new figure showing the fitted line.

- line 270: "low values are improved"? Reformulate, e.g. "Areas where  $\delta_T$  showed large negative values, show less extreme  $\delta_{RH}$ ".

We modified this sentence to

*The large difference between deserts and oceans seen in  $\delta_T$  (Fig. 3) is strongly reduced for  $\delta_{RH}$  (Fig. 7).*

- line 274: Why "basically"?

We skipped "basically".

- line 276: "weather condition [...] are usually not considered in MAX-DOAS retrieval". This sentence does not make sense, what the authors want to say is that days with such weather conditions are usually not considered for MAX-DOAS retrieval.

We have re-formulated the sentence to

*Note, however, that MAX-DOAS retrievals are usually not considered for weather conditions associated with rain and clouds.*

- line 296: I think that the 3% is not supported by the plots Fig. 8 (Fig. 7 has to be disregarded because that day was used to fit the parameters). Values of up to  $\pm 6\%$  seem more correct, but it is hard to see from the figures.

Most of the large positive deviations in Fig. 7 and 8 are related to temperature inversions, which is discussed in detail in the revised manuscript. For the discussion of possible effects of  $z_0$ , we have thus skipped profiles affected by temperature inversions. The remaining profiles with  $z_0 > 2$  km reveal a mean deviation of  $-0.5\%$  with a SD of  $1.8\%$ .

- line 300: this seems to have the wrong indentation, please check.

Lines 300 to 302 are part of the enumerate block starting at line 297, so the indentation is correct.

- line 315: add a comma after "this"

Done.

- line 317: "for" --> "at"

Done.

- line 321: Do not start sentences with "But"

We would like to ask the Copernicus language editor for a suggestion how to formulate this sentence.

- line 320 - 320: insert "order of" between "same" and "magnitude".

Done.

- line 320 - 321: This sentence is incomprehensible

We have largely revised the respective paragraph.

- Figure 9: Axis labels too small. "[...] all cycles are referred to the mean value [...]". This sentence does not make sense. Please reformulate.

We have increased the complete figure in the revised manuscript and modified the figure caption to *For better comparison, the mean value at 11:00 UTC (around solar noon for Germany) is subtracted from all datasets.*

- Figure 10: Axis labels and Axes tick labels are far too small. Please adjust the range of the x-axis of panel (c). Please check the y-axis label: Should this not be  $\delta_{RH}$ ?

We have increased font size for axis labels. The figure width was on purpose chosen as  $\frac{3}{4}$  of page width, in order to have the same subpanel size for figures 1, 5, 10, and D1 (now 1, 5, 10, 11, B3). The range of x in panel (c) was on purpose set to the same range as for (a) and (b) for better comparability. We have corrected the label of the y-axis.

In addition, we now show density plots instead of scatter plots in order to include the complete datasets in the panels.

- line 368: refer to Eq. A9 instead of Appendix A.

We moved this section to Appendix A4 and added references to the respective equations.

- Appendix B and Appendix C are never mentioned in the text.

In the revised manuscript, the Appendices about data sets have been extended, and they are now mentioned in the main text.

- line 387: remove comma after "measurements".

This paragraph has been largely revised due the addition of profiles from a climatology.

- Figure D1: axes labels are not readable. "DWD--> " and "WRF -->" seem to indicate a direction as displayed. Maybe remove the arrow, it is misleading.

We have increased font size for axis labels. We have removed the arrows from DWD and WRF. In addition, we now show density plots instead of scatter plots in order to include the complete datasets in the panels.

- line 442: add comma after "maintain".

Done.

- line 443 - 444: "This is a consequence of the spatial resolution of the WRF simulations of 1 km not resolving single mountains". This sentence seems incorrect. Reformulate.

We have re-formulated this sentence to

*This is a consequence of the spatial resolution of the WRF simulations of 1 km, which is not sufficient for resolving single mountains.*

- Figure E1: station labels are not very well readable in the figure.

We have increased the font size of station labels in Fig. E1 in the revised manuscript.

## Reply to reviewer #2

We provide a point-by-point reply to the issues raised by reviewer 2 below. The original review is included in grey. Text changes in the manuscript are indicated in italic font.

Please also note the modifications made in the revised manuscript that are specified in the Corrigendum.

The manuscript by Beirle et al. presents a parameterization of O<sub>4</sub> vertical column densities (VCD) based on surface observations of temperature (T), pressure (p), and, ultimately, relative humidity (RH). A first parameterization that only consider p and T is derived based on first principles and performs reasonably well when compared to “true” O<sub>4</sub> VCDs calculated from WRF, ECMWF, and radiosonde data. The authors use a modified version of the first-principles parameterization and the true O<sub>4</sub> VCD to develop an empirical parameterization that also include surface RH. This empirical parameterization improved the O<sub>4</sub> VCD calculations to below a 2% uncertainty that is needed for MAX-DOAS based inversions. The authors identify several instances in which the parameterization is less accurate, such as condition with surface inversions and mountainous regions.

Overall, this is a well-written manuscript that present a new method to improve O<sub>4</sub> VCD calculations. The presented parameterizations will be useful to the MAX-DOAS community, which needs these VCDs for their retrievals. There are some parts of the manuscript that could be further strengthened, as I will outline below, and a few minor text/language issues. The manuscript fits well into AMT, and I recommend its publication after minor revisions.

We thank the reviewer for the positive assessment. Below we reply to the raised issues point by point.

Detailed comments:

Line 44-45: It seems unlikely that a lapse rates close to 0 can be achieved due to condensation alone. There likely some dynamic reason as well. It may be worth citing books/manuscripts from the meteorological literature that give an overview of potential atmospheric lapse rates here.

This is a misunderstanding; we do not want to claim that the lapse rate becomes 0 by condensation. Instead, the addendum “closer to 0” is meant to indicate the direction of the change; as the dry lapse rate is negative, it is lower than the moist lapse rate, but its absolute is higher. In order to avoid confusion, we do not use “lower/higher” here. We modified the respective sentence as follows and hope that this avoids misunderstandings:

*... parts of the oceans with weaker (i.e. closer to zero) lapse rates due to condensation.*

Section 3.4: Please provide some more information on the time frame over which the sondes were flown. It also seems that some of the locations had very few sondes, thus making the statistical interpretation challenging. It may also be a good idea to add the number of sondes for each location to Table 3.

We thank the reviewer for this comment. We have added information on the time coverage of the analysed sonde launches to Appendix E. By comparison with table E1, we then noticed that the number of sonde launches did not match. Actually, table E1 lists the number of all GRUAN profiles rather than just those for SZA < 85°. We have corrected this in the revised manuscript.

We agree that for several stations, statistics are quite limited (even more for the corrected number of available profiles). However, if stations with few profiles would be skipped, some conditions (e.g. tropics) would not be included any more. We still consider the limited information content of these stations to be valuable for this study, as none of the stations shows any exceptional behaviour.

In response to the comments of reviewer 1, we have decided to present the data of table 3 in a new figure in the revised document. In order to indicate low statistics, the results for stations with few profiles are marked by lighter color.

Section 5.4 and 5.5: These sections present some interesting ideas. However, the proposed formulas are not backed up by any data or detailed analysis. I also found these sections rather distracting from the main point of the paper. They should either be expanded by showing that the calculation of lapse rates yields reasonable results by comparing them to the meteorological data the authors have already used in the manuscript or, which would be my recommendation, be moved into their own publication.

We understand that sections 5.4 and 5.5 of the discussion paper could be considered distracting. We have thus revised the manuscript as follows:

- Concerning Sect. 5.4, the effective lapse rate is now already defined in the formalism section (2.3). We now also present a comparison of the effective lapse rate to the 5 km lapse rate from ECMWF profiles in Sect. 4.
- Concerning Sect. 5.5, this is so far not more than an idea for a future application, which might indeed become a separate publication as soon as substantiated by measurements. Nevertheless, we would like to mention this idea already in this manuscript. In order not to distract the logical flow of the discussion, we moved this subsection into a new subsection of Appendix A, where the ratio of effective heights is discussed.

Lines 257 – 259: This is such a central part of the manuscript that I would recommend expanding it to provide the reader with more information on how the parameters  $a$  and  $b$  were derived. Maybe add a figure of the data and the fitting line. In addition, please provide uncertainties and  $R^2$  of the fit.

We agree that the description of the fit was lacking for detail.

In the revised manuscript, we have clarified the fitting procedure in section 2.5 (formalism).

The fit parameters (with uncertainties) are now derived in section 4.2, which also includes a new figure showing the data, correlation coefficient and the fitted line.

Line 329 – 330 (and other places in manuscript): I believe this could be generalized in stating that the parameterization loses accuracy when surface temperature inversions are present, i.e. in the morning and evening, in the Arctic, etc.

We agree. In the revised manuscript, we have added the following footnote to the introduction:

*Note that, for this approach, as well as for the parameterizations presented in this study, temperature inversions are problematic. As MAX-DOAS applications require daylight, however, night-time inversion layers are irrelevant for this study. The remaining temperature inversions at daytime, mostly occurring in early morning hours and over cold water and ice surfaces, will be discussed in Sect. 5.2.*

We discuss the effect of temperature inversions in detail in a new section (5.2) in the discussion, including a map of surface temperature inversions in ECMWF data on 18 June 2018 that clearly illustrates that for these conditions higher deviations are found.

Line 39: "... as the main source..."

Done.

Line 42: "The main reason..."

Done.

Line 159: introduce SZA here by spelling out "solar zenith angle"

Done.

Line 350-351: change to "Obviously, other factors would probably also have to be..."

Done.

# Calculating the vertical column density of O<sub>4</sub> from surface values of pressure, temperature and relative humidity

Steffen Beirle<sup>1</sup>, Christian Borger<sup>1</sup>, Steffen Dörner<sup>1</sup>, Vinod Kumar<sup>1</sup>, and Thomas Wagner<sup>1</sup>

<sup>1</sup>Max-Planck-Institut für Chemie

**Correspondence:** Steffen Beirle (steffen.beirle@mpic.de)

**Abstract.** We present a formalism that relates the vertical column density (VCD) of the oxygen collision complex O<sub>2</sub>-O<sub>2</sub> (denoted as O<sub>4</sub> below) to surface (2 m) values of temperature and pressure, based on physical laws. In addition, we propose an empirical modification which also accounts for surface relative humidity (RH). This allows for simple and quick calculation of the O<sub>4</sub> VCD without the need for constructing full vertical profiles. The parameterization reproduces the ~~real-true~~ O<sub>4</sub> VCD, as  
5 derived from vertically integrated profiles, within ~~-0.9% ± 1.0%~~ ~~-0.7% ± 1.2%~~ (mean ± SD) for WRF simulations around Germany, ~~0.1% ± 1.2%~~ ~~0.2% ± 1.8%~~ for global reanalysis data (ERA5), and ~~-0.4% ± 1.4%~~ ~~-0.3% ± 1.4%~~ for GRUAN radiosonde measurements around the world. When applied to measured surface values, uncertainties of 1 K, 1 hPa, and 16% for temperature, pressure, and RH correspond to relative uncertainties of the O<sub>4</sub> VCD of 0.3%, 0.2%, and 1%, respectively. The proposed parameterization thus provides a simple and accurate formula for the calculation of the O<sub>4</sub> VCD which is  
10 expected to be useful in particular for MAX-DOAS applications.

## 1 Introduction

In the atmosphere, two oxygen molecules can build collision pairs and dimers, which are often denoted as O<sub>4</sub> (Greenblatt et al., 1990; Thalman and Volkamer, 2013, and references therein). O<sub>4</sub> has absorption bands in the UV/visible spectral range, thus O<sub>4</sub> can be retrieved from atmospheric absorption spectra, e.g. by applying Differential Optical Absorption Spectroscopy  
15 (DOAS) (Platt and Stutz, 2008). Measurements of the O<sub>4</sub> absorption ~~pattern~~ in scattered light provide information about light path distributions in the atmosphere, for instance allowing to investigate light path ~~length~~ increase within clouds (Wagner et al., 1998) or the retrieval of cloud heights from satellite measurements (Acarreta et al., 2004; Veeffkind et al., 2016).

For Multi-Axis (MAX) DOAS, i.e. ground-based instruments measuring scattered light at different elevation angles, O<sub>4</sub> measurements provide information on vertical profiles of aerosol extinction (Heckel et al., 2005). Prerequisite for MAX-  
20 DOAS profile inversions is knowledge about the O<sub>4</sub> vertical column density (VCD) which provides the link between the measured slant column densities (SCDs) at different viewing angles and the forward modelled SCDs based on radiative transfer calculations. Thus, a wrong input of the O<sub>4</sub> VCD directly affects the resulting aerosol profiles. For the profile inversion algorithm MAPA (Beirle et al., 2019) applied to measurements taken during the CINDI-2 campaign (Kreher et al., 2020), for instance, a change of the input O<sub>4</sub> VCD of 2%, ~~3%~~, 5%, or 10% causes changes of the resulting median aerosol optical  
25 depth of 6%, ~~8%~~, 13%, or 20%, respectively. Thus, ~~for MAX-DOAS profile inversions~~, the O<sub>4</sub> VCD should be determined

with accuracy and precision better than about 3%, ~~leaving which limits the impact on resulting AODs to below 10% and leaves~~ other sources of uncertainty, i.e. the spectral analysis ( $\approx 5\%$ ) as well as radiative transfer modeling ( $\approx 4\%$ ) (see Wagner et al., 2021, Table 3 therein) as the limiting factors ~~in MAXDOAS profile inversions~~.

30 The  $O_4$  VCD can be calculated by vertical integration of the  $O_2$  number density profile squared. This requires knowledge of vertical profiles of temperature, pressure, and humidity, e.g. as derived from radiosonde measurements or meteorological models. However, ~~measured profiles-radiosonde measurements~~ are only available for few stations and do not provide continuous temporal coverage, while modelled profiles might not be available in some cases (e.g. during measurement campaigns in remote regions and poor internet connection; ~~for these cases, profiles from a climatology might be used as fallback option~~), or might not reflect the conditions at the measurement site appropriately, in particular in mountainous terrain not resolved by the model.

35 Measurements of surface air (at 2 m) temperature, pressure, and humidity, on the other hand, are routinely performed by meteorological stations, and could be added to any MAX-DOAS measurement site with relatively low costs and efforts. Wagner et al. (2019) proposed ~~a procedure how~~ to construct full temperature and pressure profiles from the respective surface values by assuming (a) a constant lapse rate of  $-6.5 \text{ K km}^{-1}$  from ground up to 12 km, and constant temperature above, and (b) applying the barometric formula.<sup>1</sup> Wagner et al. (2019) estimate the uncertainty of the calculated  $O_4$  VCD to 3% and list the  
40 diurnal variation of the surface temperature and the limited representativeness of the surface temperature for the temperature profile above the boundary layer as ~~the~~ main source of uncertainty.

The method proposed by Wagner et al. (2019) reproduces the true  $O_4$  VCD within about 2% (~~mean-bias~~)  $\pm 2\%$  standard deviation (SD) globally when compared to ECMWF profiles, ~~as shown below~~. Locally, however, large deviations up to 7% could be found. ~~Main reason for systematic deviations to the true VCD turned out to be the~~, ~~as shown in this study, which is~~  
45 ~~mainly caused by the~~ assumption of a fixed lapse rate of  $-6.5 \text{ K km}^{-1}$ ; While this value reflects typical continental conditions quite well, it is not appropriate in particular over deserts, where lapse rates are stronger (closer to the dry adiabatic lapse rate), and ~~large~~ parts of the oceans with weaker ~~lapse rates (closer to 0 (i.e. closer to zero) lapse rates~~ due to condensation).

In this paper we present a simpler approach for the calculation of  $O_4$  VCD just from surface values of temperature and pressure and an a-priori lapse rate based on physical laws, without the need of constructing full profiles. In addition, we  
50 provide an empirical parameterization involving surface relative humidity that also accounts for variations of the atmospheric lapse rate. The final equation allows for simple and quick calculation of the  $O_4$  VCD with high accuracy and precision just from surface measurements of temperature, pressure, and relative humidity.

The manuscript derives the formalism of the parameterizations of the  $O_4$  VCD in ~~section Sect. 2~~. In ~~section Sect. 3~~, the datasets used for illustration and quantification of uncertainties are introduced, followed by applications of the  $O_4$  parameteri-  
55 zations in ~~section Sect. 4~~. Important aspects like ~~accuracy/precision, diurnal cycle, or the dependency on comparison to standard methods used for the calculation of the~~  $O_4$  VCD, ~~the impacts of temperature inversions~~, surface altitude, ~~or diurnal cycles, and the accuracy and precision of the proposed parameterizations~~ are discussed in ~~section Sect. 5~~, followed by conclusions.

---

<sup>1</sup> ~~Note that, for this approach, as well as for the parameterizations presented in this study, temperature inversions are problematic. As MAX-DOAS applications require daylight, however, night-time inversion layers are irrelevant for this study. The remaining temperature inversions at daytime, mostly occurring in early morning hours and over cold water and ice surfaces, will be discussed in Sect. 5.2.~~

## 2 Formalism

In this section, we provide the formalism for the calculation of O<sub>4</sub> VCDs from surface values of pressure, temperature, and relative humidity.

### 2.1 Notation

Basic quantities of the derivation below are (a) the number density  $n$ , and (b) the vertical column density (VCD)  $V$ , i.e. the vertically integrated number density.

The O<sub>4</sub> number density is just defined as the O<sub>2</sub> number density squared. Consequently, the O<sub>4</sub> number density has the unit molecules<sup>2</sup> cm<sup>-6</sup>, and the O<sub>4</sub> VCD has the unit molecules<sup>2</sup> cm<sup>-5</sup>. This matches the common procedure in the DOAS community; the O<sub>4</sub> cross section is given in cm<sup>5</sup> molecules<sup>-2</sup> accordingly (Greenblatt et al., 1990; Thalman and Volkamer, 2013).

Pressure is denoted by  $p$ , temperature by  $T$ , and the altitude above sea level by  $z$ , while altitude above ground level is denoted by  $z'$ . For relative humidity, RH is used in the text as well as in formulas. Surface values are indicated by the subscript "0". Quantities related to O<sub>2</sub> and O<sub>4</sub> are indicated by a respective subscript. For a full list of quantities and symbols see [Tables 1 and 2](#).

**Table 1.** Variables used in this study. A subscript of 0 indicates surface values for  $n, p, T, z, p, T, z,$  or RH.

Quantity	<del>Abbreviation</del> <u>Acronym</u>	Symbol	Unit
Number density	-	$n_{O_2}$	molecules cm <sup>-3</sup>
		$n_{O_4}$	molecules <sup>2</sup> cm <sup>-6</sup>
Vertical column density	VCD	$V_{O_2}$	molecules cm <sup>-2</sup>
		$V_{O_4}$	molecules <sup>2</sup> cm <sup>-5</sup>
Pressure	-	$p$	hPa
Temperature	-	$T$	K
Altitude above sea level	-	$z$	m
Altitude above surface	-	$z'$	m
Effective height	-	$h$	m
Scale height	-	$H$	m
Relative humidity	RH	RH	
<del>Effective tropospheric lapse</del> <u>Lapse</u> rate	-	$\Gamma$	K km <sup>-1</sup>
Relative deviation <del>between of parameterized and to</del> true O <sub>4</sub> VCD	-	$\delta$	%
Top of atmosphere <sup>a</sup>	TOA	$z_{TOA}$	m
<del>(here: highest available profile layer)</del> Total column water vapor	TCWV	$V_{H_2O}$	molecules cm <sup>-2</sup>

<sup>a</sup> here: highest available/possible profile layer.

**Table 2.** Constants used in this study. Numbers are listed with 6 digits.

Quantity	Symbol	Value	Unit
Gravitational acceleration on Earth	$g$	9.80665 <sup>a, b</sup>	$\text{m s}^{-2}$
Molar mass of dry air	$M$	0.0289655 <sup>a</sup>	$\text{kg mol}^{-1}$
Universal gas constant	$R$	8.31446 <sup>a</sup>	$\text{J K}^{-1} \text{mol}^{-1}$
O <sub>2</sub> volume mixing ratio in dry air	$\nu_{\text{O}_2}$	0.209392 <sup>b, c</sup>	
Combined constants (eqEq. 11)	$C$	$0.0185646 \text{ K Pa}^{-2} \text{ mol}^2 \text{ m}^{-5} 6.73266 \text{ e}+39 \cdot 10^{39}$	$\text{K hPa}^{-2} \text{ molecules}^2 \text{ cm}^{-5}$

<sup>a</sup> from the Python module MetPy (May et al., 2021).

<sup>b</sup> latitudinal variations of  $g$  are below  $\pm 0.27\%$  and are neglected in this study.

<sup>c</sup> from Tohjima et al. (2005)

## 2.2 General approach

The VCD  $V$  is the vertically integrated number density  $n$ :

$$V = \int_{z_0}^{\infty} n(z) dz \quad (1)$$

75 This integral can be re-written as

$$V = n_0 \cdot h, \quad (2)$$

with

$$h = \int_{z_0}^{\infty} \frac{n(z)}{n_0} dz \quad (3)$$

This effective height  $h$  can be understood as the height of the gas column if the gas would be in a homogenous box under surface conditions  $p_0$  and  $T_0$ . Note that the effective height equals the scale height  $H$  only in case of exponential profiles, i.e. an isothermal atmosphere (see Appendix A).

Thus, the VCDs for O<sub>2</sub> and O<sub>4</sub> can be written as

$$V_{\text{O}_2} = n_{\text{O}_2,0} \cdot h_{\text{O}_2} \quad (4)$$

and

$$85 \quad V_{\text{O}_4} = n_{\text{O}_4,0} \cdot h_{\text{O}_4} = n_{\text{O}_2,0}^2 \cdot h_{\text{O}_4} \quad (5)$$

Re-arranging eqEq. 4 for  $n_{\text{O}_2,0}$  and replacing one  $n_{\text{O}_2,0}$  term in eqEq. 5 yields

$$V_{\text{O}_4} = V_{\text{O}_2} \cdot n_{\text{O}_2,0} \cdot \frac{h_{\text{O}_4}}{h_{\text{O}_2}} \quad (6)$$

Hence the  $O_4$  VCD can be expressed as the product of the  $O_2$  VCD, the  $O_2$  surface number density, and the ratio of effective heights of  $O_2$  and  $O_4$  profiles. So far, no simplifications or approximations were made, thus Eq. 19 holds for any atmospheric conditions.

### 2.3 $O_4$ VCD as a function of surface pressure, surface temperature, and lapse rate

Based on eq. 6, the  $O_4$  VCD can be related to surface pressure, surface temperature, and lapse rate, if some further assumptions are made:

1. Assuming a hydrostatic atmosphere, the surface pressure is just the gravitational force per area of the total air column. Thus, the  $O_2$  VCD, i.e. the vertically integrated column, VCD is directly related to the surface pressure:

$$V_{O_2} = \frac{\nu_{O_2}}{g \cdot M} \cdot p_0, \quad (7)$$

with  $\nu_{O_2}$  being the volume mixing ratio of  $O_2$  in dry air,  $g$  being the gravitational acceleration on Earth, and  $M$  being the molar mass of dry air.

2. According to the ideal gas law for dry air, the surface number density of  $O_2$  can be expressed as

$$n_{O_2,0} = \frac{\nu_{O_2}}{R} \cdot \frac{p_0}{T_0}, \quad (8)$$

with the universal gas constant  $R$ .

3. The ratio of effective heights for  $O_2$  and  $O_4$  depends on the actual profile shape for  $O_2$ . For some specific cases, the integral (eq. in Eq. 3) can be solved analytically, as shown in Appendix A. (see Appendix A for details):

- For an isothermal atmosphere, i.e. an exponential profile of  $n_{O_2}$ , the ratio  $\frac{h_{O_2}}{h_{O_4}}$  is just 2. For the more realistic assumption of 2 (Eq. A2).
- For a constant lapse rate  $\Gamma$ , the ratio becomes  $2 + \frac{R}{g \cdot M} \Gamma$  (Eq. A10).
- For real atmospheric conditions, where the lapse rate varies with altitude, the ratio of effective heights can be still described by Eq. A10 if an effective lapse rate is considered:

$$\Gamma_{\text{eff}} := \left( \frac{h_{O_2}}{h_{O_4}} - 2 \right) \cdot \frac{g \cdot M}{R} \quad (9)$$

For a given atmospheric profile, the effective lapse rate is thus defined as the lapse rate of a polytropic atmosphere of the same  $O_4$  VCD.

Replacing these terms in eq. 6 yields

$$\begin{aligned} V_{O_4,\Gamma} &= \frac{\nu_{O_2}^2}{R \cdot g \cdot M} \left/ \left( 2 + \frac{R}{g \cdot M} \Gamma \right) \cdot \frac{p_0^2}{T_0} \right. \\ &= \frac{C}{2 + \frac{R}{g \cdot M} \Gamma} \cdot \frac{p_0^2}{T_0} \end{aligned}$$

Replacing the terms in Eq. 6 by Eq. 7, Eq. 8 and Eq. A10 yields

$$\begin{aligned}
 V_{O_4, \Gamma} &= \frac{\nu_{O_2}^2}{R \cdot g \cdot M} \left/ \left( 2 + \frac{R}{g \cdot M} \Gamma \right) \cdot \frac{p_0^2}{T_0} \right. \\
 &= \frac{C}{2 + \frac{R}{g \cdot M} \Gamma} \cdot \frac{p_0^2}{T_0}
 \end{aligned} \tag{10}$$

with

$$C = \frac{\nu_{O_2}^2}{R \cdot g \cdot M} \tag{11}$$

combining the constant factors.-

Thus with the assumptions specified above, combining the constant factors. Thus with the assumptions specified above, the  
 120  $O_4$  VCD is proportional to  $p_0^2/T_0$ , with the lapse rate VCD is proportional to  $p_0^2/T_0$ , with the lapse rate  $\Gamma$  determining the slope.-

## 2.4 VCD as function of surface pressure, surface temperature, and surface humidity

So far, the formalism was based on dry air. Humid air is lighter than dry air, and contains less . Thus, humidity affects the  
 vertical profile and hence all factors of eq. 6, i.e. the VCD, the surface number density, and the effective heights of and  
 125 determining the slope.

As the vertical humidity profile is generally not well known, these effects cannot be described analytically. In order to still  
 have a simple parameterization of the VCD based on surface measurements, we follow an empirical approach and introduce a  
 modification of eq. ?? involving surface humidity.-

As shown in section ??, the VCD is closely related to the *relative* humidity at ground, while no correlation to *specific*  
 130 humidity was found. This was surprising on first glance, as the effect of humidity on number density should be better described  
 by specific humidity. However,  $RH_0$  is closely related to the effective lapse rate of the lower troposphere, which has a strong  
 impact in eq. ?. This will be discussed in more detail in section ??.-

The parameterization of the VCD from surface values  $p_0$ ,  $T_0$ , and  $RH_0$  was thus chosen such that a linear function of  $RH_0$   
 replaces the linear function of  $\Gamma$  in the denominator of eq. ??.-

$$135 \quad V_{O_4, RH} = \frac{C}{a + b \cdot RH_0} \cdot \frac{p_0^2}{T_0},$$

The parameters were derived as  $a = 1.769$  and  $b = 0.1257$  by a least squares fit based on ECMWF profiles for 18 June 2018  
 (see section ??). This allows for simple calculation of the VCD as-

$$V_{O_4, RH} = \frac{6.733 \cdot 10^{39}}{1.769 + 0.1257 \cdot RH_0} \cdot \frac{p_0^2}{T_0} \text{ molec}^2 \text{ cm}^{-5}.$$

for  $RH$  as dimensionless number (i.e., 0.5 for 50% RH),  $p_0$  in , and  $T_0$  in .

140 Note that while this empirical approach basically parameterizes the effective lapse rate by  $RH_0$ , also the effect of humid air  
 being lighter is , at least partly, implicitly accounted for by the empirical fit.-

## 2.4 Calculation of the “true” O<sub>4</sub> VCD

In section 4, we investigate In order to evaluate the performance of the different parameterizations for the O<sub>4</sub> VCD for modelled and measured profiles. For this purpose, we compare the results of eq. ?? and eq. 20 to the, we also calculate the “true” O<sub>4</sub>

145 VCD, which is derived by

(a) calculating the profile of  $n_{\text{O}_2}$  from profiles of  $T$ ,  $p$  and  $\text{RH}$ , fully considering the effects of humidity, and. In this step, the effect of humidity is explicitly accounted for by subtracting the water vapor pressure before calculating  $n_{\text{O}_2}$  based on the ideal gas law.

(b) performing the numerical integration (using Simpson’s rule) of  $n_{\text{O}_2}^2$  from surface to top of atmosphere (TOA).

150 The integration has to be performed up to sufficiently high altitudes (Wagner et al. (2019) recommend  $z_{\text{TOA}} \geq 30$  km) as otherwise the integrated VCD would be biased low due to the missing column above. As not all datasets considered below cover this altitude range, we estimate and correct for the missing O<sub>4</sub> column above the highest profile level by applying eq. ?? Eq. 10 for the highest available layer, assuming a lapse rate of zero above. Note that the temperature increase in the upper stratosphere is not relevant here as the contribution to the O<sub>4</sub> VCD above 30 km is negligible. Thus, the “true” O<sub>4</sub> VCD is  
155 calculated as

$$V_{\text{O}_4, \text{true}} = \int_{z_0}^{z_{\text{TOA}}} n_{\text{O}_2}^2(z) dz + \frac{C}{2} \cdot \frac{p_{\text{TOA}}^2}{T_{\text{TOA}}} \quad (12)$$

For  $z_{\text{TOA}}$  of 20 km, the correction term is of the order of 0.3% of the total O<sub>4</sub> column.

## 2.5 O<sub>4</sub> VCD as a function of surface pressure, surface temperature, and surface relative humidity

Equation 10 might be applied for a common lapse rate, like  $-6.5 \text{ K km}^{-1}$  as proposed in Wagner et al. (2019). This works  
160 generally well over most continental regions. However, large deviations have to be expected for regions with different lapse rates, in particular over deserts, where lapse rates are typically stronger (more negative, i.e. close to the dry adiabatic lapse rate). Over parts of the ocean, on the other hand, lapse rates are weaker (closer to zero).

In order to modify Eq. 10 such that it can be applied globally, but keep it still a simple function of surface measurements, we make use of the relation between the effective lapse rate and the RH at ground:

- 165
- For ascending air masses,  $\text{RH}_0$  determines the altitude at which condensation takes place. This relation is directly reflected in the calculation of the lifted condensation level (LCL) as function of  $\text{RH}_0$  (Lawrence, 2005; Romps, 2017). Thus, the lower  $\text{RH}_0$ , the higher the altitude range above ground where dry adiabatic lapse rates apply.
  - For descending air masses (in particular the large-scale subsidence over tropical deserts), no condensation takes place and dry adiabatic lapse rates apply.

170 In both cases, low relative humidity at ground is associated with lapse rates closer to the dry adiabatic lapse rate.

Real atmospheric profiles are of course more complex as these simplified scenarios, in particular due to advection, but still, a correlation between  $\text{RH}_0$  and effective lapse rates is expected. We thus parameterize the effective lapse rate by the relative

humidity at ground via a linear function:

$$\Gamma_{\text{eff}} = \alpha + \beta \cdot \text{RH}_0 \quad (13)$$

175 Replacing this in Eq. 10 results in  $V_{\text{O}_4}$  becoming a function of surface values for pressure, temperature, and relative humidity:

$$\begin{aligned} V_{\text{O}_4, \text{RH}} &= \frac{C}{2 + \frac{R}{g \cdot M} \cdot (\alpha + \beta \cdot \text{RH}_0)} \cdot \frac{p_0^2}{T_0} \\ &= \frac{C}{a + b \cdot \text{RH}_0} \cdot \frac{p_0^2}{T_0}, \end{aligned} \quad (14)$$

where the parameters  $a$  and  $b$  are linked to  $\alpha$  and  $\beta$  from Eq. 13 via

$$\alpha = (a - 2) \cdot \frac{g \cdot M}{R} \quad (15)$$

and

$$180 \quad \beta = \frac{g \cdot M}{R} \cdot b. \quad (16)$$

The parameters  $a$  and  $b$  can then be determined by a linear least squares fit by comparing  $V_{\text{O}_4, \text{RH}}$  to  $V_{\text{O}_4, \text{true}}$ :

$$V_{\text{O}_4, \text{RH}} = \frac{C}{a + b \cdot \text{RH}_0} \cdot \frac{p_0^2}{T_0} \stackrel{!}{=} V_{\text{O}_4, \text{true}}, \quad (17)$$

thus

$$a + b \cdot \text{RH}_0 \stackrel{!}{=} \frac{C}{V_{\text{O}_4, \text{true}}} \cdot \frac{p_0^2}{T_0} =: Q. \quad (18)$$

185  $a$  and  $b$  will be derived in Sect. 4.2 based on true  $\text{O}_4$  VCDs calculated from ECMWF profiles. This empirical approach also, at least partly, corrects for effects neglected in the derivation of Eq. 10, i.e. ignoring the tropopause in the calculation of the ratio of effective heights (App. A3), and applying the ideal gas law for dry air in Sect. 2.3.

190 From  $a$  and  $b$ , also the corresponding effective lapse rate for a given  $\text{RH}_0$  can then be calculated with Equations 13, 15 and 16. This lapse rate allows to construct full atmospheric profiles of  $T$  and  $p$  (applying the barometric formula for polytropic atmosphere) from surface measurements when needed, in particular for MAX-DOAS inversions based on optimal estimation. As humidity effects are already accounted for in the determination of  $a$  and  $b$ , no further correction for humidity should be applied in this case.

## 2.6 Comparison of parameterized to “true” $\text{O}_4$ VCD

In order to assess accuracy and precision of the proposed calculation of the  $\text{O}_4$  VCD from surface measurements of  $T_0$ ,  $p_0$  and  $\Gamma$  (Eq. 10) or  $\text{RH}_0$  (Eq. 14), we define the relative deviation  $\delta$  of parameterized-a derived  $\text{O}_4$  VCDs to the true value:

$$\delta_{\Gamma, x} = \frac{V_{\text{O}_4, \Gamma} - V_{\text{O}_4, \text{true}}}{V_{\text{O}_4, \text{true}}} \frac{V_{\text{O}_4, x} - V_{\text{O}_4, \text{true}}}{V_{\text{O}_4, \text{true}}} \quad (19)$$

and

$$\delta_{\text{RH}} = \frac{V_{\text{O}_4, \text{RH}} - V_{\text{O}_4, \text{true}}}{V_{\text{O}_4, \text{true}}}$$

200 Deviations  $\delta_T$  and  $\delta_{\text{RH}}$  are presented below (section 4) as frequency distributions or as mean  $\mu$  and SD  $\sigma$ . The index  $x$  indicates the  $\text{O}_4$  VCD dataset and is “T” for  $V_{\text{O}_4, \text{T}}$  and “RH” for  $V_{\text{O}_4, \text{RH}}$ .

### 3 Datasets

We For illustration as well as for the quantification of uncertainties, we apply the derived formalism to atmospheric datasets for illustration and uncertainty estimates below. For this purpose, we use different datasets: different atmospheric datasets:

1. Global model data, in order to check for the performance of the parameterizations globally, covering the full range of the input-relevant parameter space for surface values of pressure, temperature, humidity, and altitude.
2. Regional model data with high spatial resolution, which is are also compared to surface stations and allows to investigate allow to investigate the impact of diurnal cycles.
3. Balloon-borne radiosonde measurements, in order to apply the formalism to high-resolved profile measurements.

210 Nighttime profiles of  $T$  can be considerably different from daytime profiles, in particular in case of temperature inversions (i.e. positive lapse rates) often occurring within the nocturnal boundary layer. For MAX-DOAS measurements, however, these eases nighttime profiles are irrelevant. Thus, we consider all atmospheric datasets for daytime conditions only. This is done by selecting data for  $\text{SZA} < \text{with an solar zenith angle (SZA) below } 85^\circ$ .

#### 3.1 Global model (ECMWF)

We use global model data as provided by the European Centre for Medium-Range Weather Forecasts (ECMWF) for two purposes:

- In order to investigate global patterns, we use ERA5 reanalysis data (Hersbach et al., 2020) with a truncation at T639 and truncated at wavenumber 639 on the Gaussian grid N320, corresponding to  $\approx 0.3^\circ$  resolution. Model output is provided hourly. Here, we focus on ERA5 data for four selected days, i.e. the 18 June, 18 March, 18 September and 18 December 2018, covering the full globe (note that for each day, the polar region of hemispheric winter is not covered due to the SZA selection) for all seasons. As the regular latitude-longitude grid over-represents high latitudes, we only consider the fraction of  $\cos(\text{lat})$  pixels for each latitude for the calculation of histograms, correlation coefficients, means and standard deviations.
- For comparison with radiosonde profiles (see below) the standard approach for the calculation of the  $\text{O}_4$  VCD that was used in MAPA so far, we use ERA-Interim reanalysis data with a truncation at T255 truncated at wavenumber 255,

225 corresponding to  $\approx 0.7^\circ$  resolution. ~~A preprocessed dataset was created where the~~, which was preprocessed to a dataset  
with 6 hourly model output (0:00, 6:00, 12:00, 18:00 UTC) ~~was~~ interpolated to a regular horizontal grid with a resolution  
of  $1^\circ$ . ~~From this, profile data is interpolated to the radiosonde launch in space and time. The reason for also including this~~  
~~rather coarsely resolved model data was that we also use the same dataset and interpolation procedure as default for the~~  
230 ~~extraction of ECMWF profiles at our MAX-DOAS instruments and the calculation of the VCD within profile inversions~~  
~~with MAPA (Beirle et al., 2019)~~ This dataset is denoted as ERA\_I<sub>daily</sub> below.

In addition, we make use of a monthly climatology of atmospheric profiles (ERA\_I<sub>clim</sub>) based on the same ERA-Interim  
data, which was constructed as back-up solution recommended within the FRM4DOAS project in case of no other profile  
information being available.

### 3.2 Regional model (WRF-Chem) and surface measurements (DWD)

235 We use the Weather Research and Forecasting (WRF) model version 4.2 (Skamarock et al., 2019) for high resolution ~~simulation~~  
( $3 \times 3 \text{ km}^2$ ) simulations of meteorological parameters (including  $T$ ,  $p$  and RH) around Germany. ~~A nested domain centred~~  
~~at  $49.12^\circ\text{N}$ ,  $10.20^\circ\text{E}$  was set up in Lambert conformal conic (LCC) projection with coarser domain (d01) at  $15 \times 15 \text{ km}^2$~~   
~~horizontal resolution and finer domain (d02) at  $3 \times 3 \text{ km}^2$  resolution (fig. B1). Vertically the model extends from surface until~~  
~~50 with 42 terrain following layers in between. The spatial extent of the d01 domain is  $4800 \times 3416 \text{ km}^2$  while that for d02~~  
240 ~~is  $1578 \times 1473 \text{ km}^2$ . The model simulations were set up for a two months period (May & June) in~~ for May and June 2018.  
Further details on the WRF model set-up are provided in Appendix B1.1.

~~We use the ERA5 reanalysis dataset with a horizontal resolution  $0.25^\circ \times 0.25^\circ$  and a temporal resolution of 3 hours, downloaded~~  
~~at pressure levels and at the surface for constraining the meteorological initial and lateral boundary conditions. The soil~~  
~~classification, terrain height, and land use patterns were taken from the 21 category Noah-modified IGBP-MODIS land use~~  
245 ~~data.~~

~~Here we focus on WRF data for 1-9 May 2018 in the domain d02. The selection of  $SZA < 85^\circ$  results in a daily coverage~~  
~~from 6:00 h to 17:00 h UTC for each day. The vertical profiles reach up to a pressure level of 50 hPa, corresponding to an~~  
~~altitude of about 20 km. The missing part of the atmosphere contributes about 0.3% to the total VCD. This effect is considered~~  
~~accordingly in the calculation of the true VCD (see section ??).~~

### 250 3.3 Surface measurements

WRF simulations of surface values are also compared to surface measurements performed by Germany's National Meteorological  
Service (Deutscher Wetterdienst, DWD) ~~provides hourly measurements of surface temperature, pressure and relative~~  
~~humidity for a network of ground stations in Germany (Kaspar et al., 2013). Data are provided via the climate data center~~  
~~web interface (CDC-v2.1; ). The meteorological measurements are performed in accordance to the guidelines of the world~~  
255 ~~meteorological organization (WMO) to minimize local effects. Additionally we have applied quality control filters such that the~~

parameters  $QUALITAETS\_BYTE$  (QB)  $< 4$  and  $QUALITAETS\_NIVEAU$  (QN) is either 3 (automatic control and correction) or 7 (second control done, before correction) to only retain the measurements of highest quality.

260 For this study, we only consider DWD stations providing  $T_0$ ,  $p_0$ , and  $RH_0$  simultaneously, resulting in 206 stations which are displayed in fig. B1. We select measurements for the time period covered by the WRF simulations in order to quantify accuracy and precision of the WRF simulations of surface values. In particular, we investigate how far WRF reflects the diurnal pattern of surface properties.

In Appendix B0.1, a comparison of surface values from WRF to the station network is shown, revealing that the surface temperatures modeled by WRF are biased low by 1 K on average, while RH surface values are biased high by 7%. [For further details see Appendix B0.1 and B0.1.](#)

### 265 3.3 Radiosonde measurements (GRUAN)

The Global Climate Observing System (GCOS) Reference Upper-Air Network (GRUAN) is an international reference observing network of sites measuring essential climate variables above Earth's surface (Sommer et al., 2012; Bodeker et al., 2016). Atmospheric profiles of temperature, pressure, and humidity are measured by regular balloon soundings equipped with radiosondes and water vapor measurements (Dirksen et al., 2014). Here we use the RS92 GRUAN Data Product Version 2 (RS92-GDP.2), focusing on certified stations. Vertical profiles and surface values of pressure, temperature and relative humidity are taken directly from the level-2 files for each launch. Further information on the GRUAN stations used in this study are provided in Appendix B1.

## 4 Application to atmospheric datasets

In this section, we apply the parameterizations [if of the  \$O\_4\$  VCD derived in section Sect. 2 to modeled and measured atmospheric datasets.](#) [We first apply eq. ?? in section ??, and assess the accuracy and precision of the different parameterizations by comparison to the true  \$O\_4\$  VCD \(Sect. 2.4\). We first present  \$O\_4\$  VCDs based on an a priori lapse rate in Sect. 4.1, discuss the impact of humidity in section ??, and apply eq. 20 involving also relation between effective lapse rate and surface humidity in Sect. 4.2, and finally present  \$O\_4\$  VCDs based on  \$RH\_0\$  in section ??.](#) [Sect. 4.3.](#)

### 4.1 $O_4$ VCD as a function of $p_0$ , $T_0$ , and lapse rate $\Gamma$

280 [According to eq. ??](#) [According to Eq. 10](#), the  $O_4$  VCD is proportional to  $p_0^2/T_0$ , with the lapse rate  $\Gamma$  determining the slope. We illustrate this correlation for the investigated datasets [as shown](#) in Fig. [??](#)1.

[For  \$V\_{O\_4, true}\$  varies considerably for all datasets, a very good correlation between  \$p\_0^2/T\_0\$  and  \$V\_{O\_4, true}\$  \(see sect. ??\) is where the low values are caused by mountains due to reduced pressure, while the very high values for ERA5 and GRUAN are caused by cold temperatures in polar regions. The variability of  \$V\_{O\_4, true}\$  is well reflected in  \$p\_0^2/T\_0\$ , and very good correlation between both quantities are found, with most \[datapoints matching data points in accordance\]\(#\) to plausible lapse rates in the range of  \$-4\$  to  \$-6.5\$  K km \$^{-1}\$ . For the WRF simulations for Germany, \[highest correlation is found, with\]\(#\) most data points \[are\]\(#\) matching to](#)

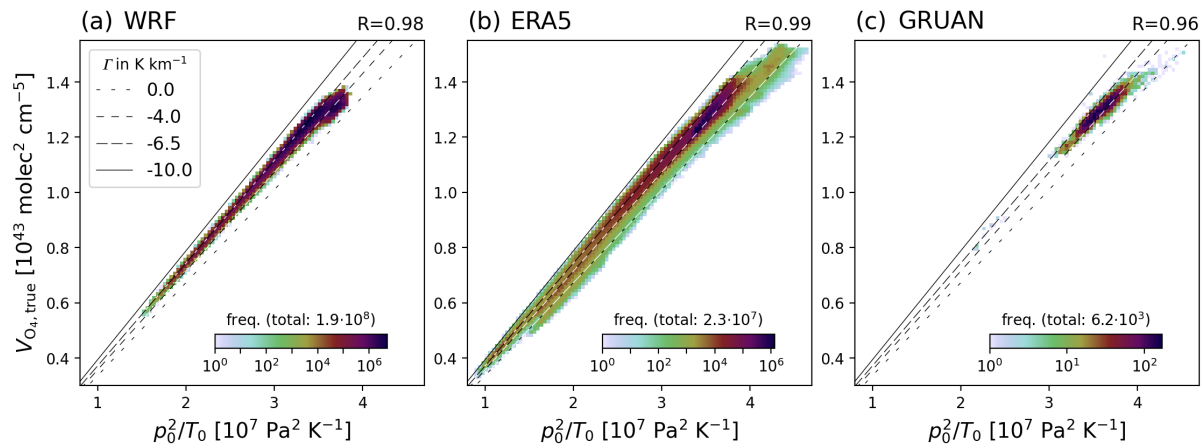


**Figure 1.** Relation-Density plots of the relation between the  $O_4$  VCD to  $p_0^2/T_0$  and the expected dependency according to eq. 10 for different lapse rates (colored lines) for (a) WRF data on 1 for May, 12 to June 2018 from 7:00 to 17:00 UTC, (b) ECMWF-ERA5 data on 18 June for the 4 selected days in 2018, 12:00 UTC, and (c) all available GRUAN profiles. For (a) and (b), only 1% Respective correlation coefficients are provided in the top right of each panel. Lines display the data is plotted in order expected dependency according to keep the figure readable Eq. 10 for different lapse rates. Low values correspond to mountainous high altitude sites with low surface pressure; for GRUAN, only few of such stations are available (Boulder and La Reunion at 1.7 km and 2.2 km altitude, respectively). The very high values for ERA5 and GRUAN are observed for the station Barrow (Alaska) for very low polar regions with cold temperatures (down to  $< 240$  K) in spring.

a lapse rate close to  $-6.5$  K  $km^{-1}$ . ECMWF-ERA5 and GRUAN data show higher variability in slopes, as they also cover a wider range of atmospheric conditions. For all datasets, the low values are caused by mountains due to reduced pressure. For the GRUAN measurements, the highest values are observed for Barrow ( $71.32^\circ N$ ), associated with very cold temperatures in spring.

Wagner et al. (2019) proposed to determine the  $O_4$  VCD based on vertical profiles of  $T$  and  $p$  constructed from the respective surface values by assuming a constant tropospheric lapse rate of  $-6.5$  K  $km^{-1}$ . We can use eq. 10 for the same purpose, but without the need for constructing full vertical profiles. Note that both methods yield almost the same results, as also the physical assumptions are the same (hydrostatic pressure, ideal gas, dry air, adiabatic lapse rate). The only difference is that Wagner et al. (2019) assumed a tropopause at 12 km, with constant  $T$  above, while in the calculation of the ratio of effective heights (see Appendix A),  $\Gamma$  is assumed to be constant throughout the atmosphere, resulting in a small overestimation of eq. 10 of about 0.5% compared to the procedure described in Wagner et al. (2019).

Figures 2 and 3 display maps of the deviation  $\delta_\Gamma$  between parameterized and true  $O_4$  VCD for WRF and ECMWF-ERA5, respectively, assuming a constant a-priori lapse rate of  $-6.5$  K  $km^{-1}$ . Results for additional days for ERA5 are shown in Appendix C.

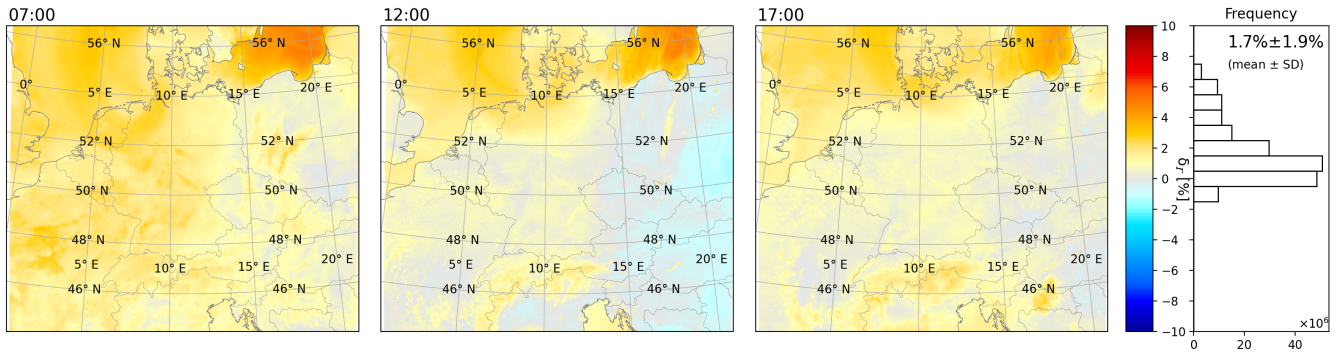


**Figure 2.** Deviation  $\delta_{\Gamma}$  according to eqEq. ??-19 for WRF simulations at 7:00, 12:00, and 17:00 UTC on 1 May 2018. On the right, the frequency distribution of  $\delta_{\Gamma}$  and its mean and SD are given for the WRF simulation period from 1 to 9 May to June 2018.

Within the WRF domain d02, a generally Generally, good agreement between  $V_{O_4, \Gamma}$  and  $V_{O_4, true}$  is found (Fig. ??). On 2); on average,  $\delta_{\Gamma}$  is 1.5%1.7%, i.e.  $V_{O_4, \Gamma}$  are higher than  $V_{O_4, true}$  by 1.5%1.7%. Over land around noon,  $\delta_{\Gamma}$  is close to 0. Over ocean, however,  $\delta_{\Gamma}$  is generally higher (up to 6%higher (about 3% up to 7%).

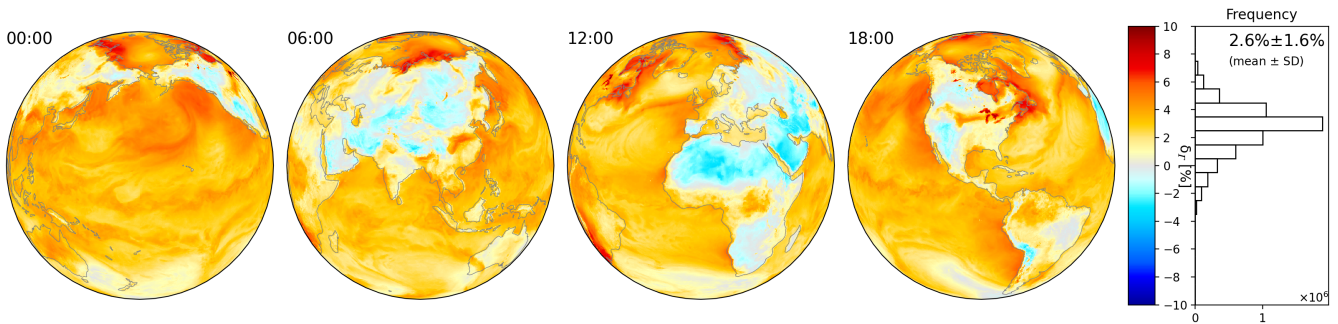


**Figure 3.** Deviation  $\delta_{\Gamma}$  according to eqEq. ??-19 for ECMWF-ERA5 at 0:00, 6:00, 12:00 and 18:00 UTC on 18 June 2018. The projection focuses on daytime for each timestep. On the right, the frequency distribution and mean and SD are given for all hourly outputs from 18 June 2018. Respective deviations for days in other seasons are shown in Fig. C1.

305 Deviation according to eq. ?? for ECMWF at 0:00, 6:00, 12:00 and 18:00 UTC on 18 December 2018. The projection focuses on daytime for each timestep. On the right, the frequency distribution and mean and SD are given for all hourly outputs from 18 December.

310 Also for ECMWF For ERA5 data on 18 June 2018,  $\delta_{\Gamma}$  over Germany is close to 0 as well (Fig. ??3). On global scale, however, only moderate agreement is found between  $V_{O_4, \Gamma}$  and  $V_{O_4, true}$ , with a mean value deviation of 2.6%and 2.8% for in June and December, respectively. High values for  $\delta_{\Gamma}$  are found generally over ocean. For In particular over cold water surfaces, like the West coast of North and South America, the Hudson Bay, or the Great lakes,  $\delta_{\Gamma}$  is very high (up to 7%).

This is related to temperature inversions close to ground: due to the too low surface temperatures, the  $O_4$  VCD calculated from Eq. 10 is biased high. This will be discussed in detail in Sect. 5.2. Over continents,  $\delta_\Gamma$  is closer lower, and generally close to 0, but particularly except over deserts, where negative values are observed. If the VCD is calculated as proposed by Wagner et al. (2019), the deviations show the same patterns, with slightly lower means (due to consideration of the tropopause) but same SD. These

## 4.2 Effective lapse rate and relative humidity at ground

Figure 4 displays the effective lapse rate, as defined in Eq. 9, for ERA5 data from 18 June 2018, clearly showing that the general patterns of systematic deviations from 0 seen in Fig. 3 are mainly caused by the simple assumption of a globally constant lapse rate in the calculation of  $\delta_\Gamma$ .

## 4.3 Effects of humidity

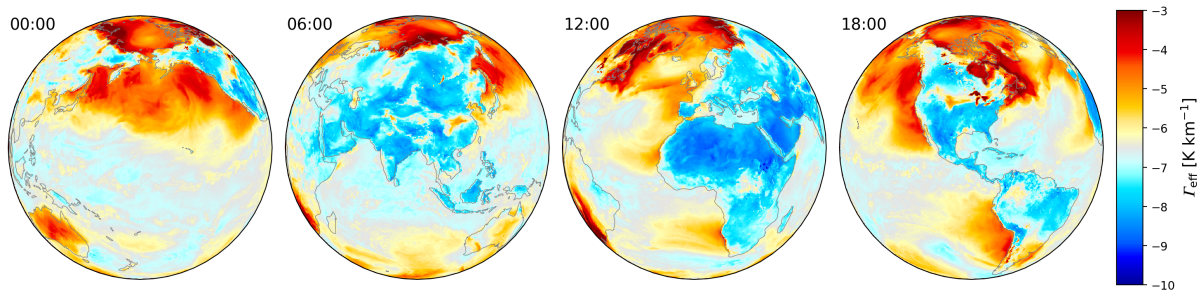
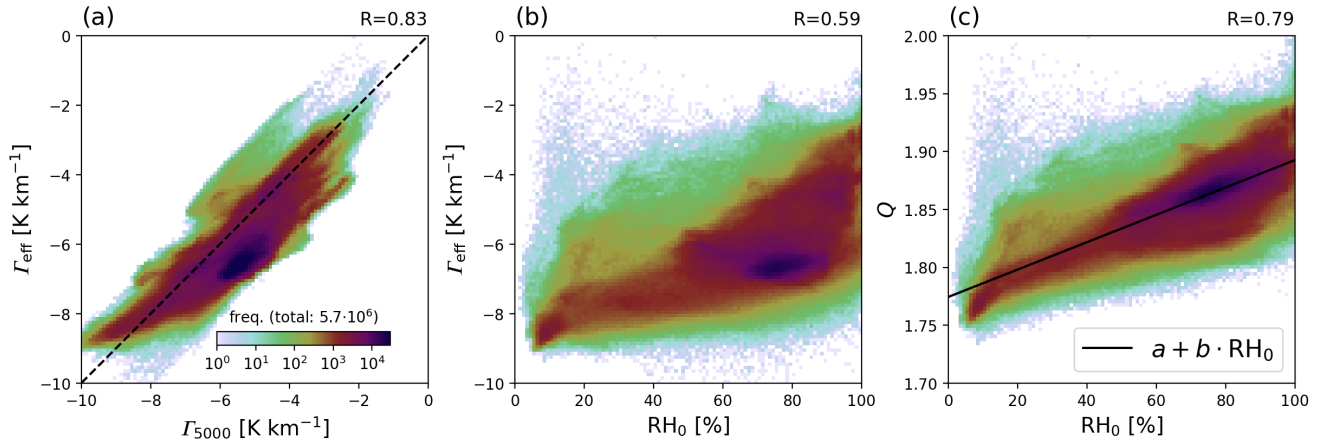


Figure 4. Effective lapse rate  $\Gamma_{\text{eff}}$  as defined in Eq. 9 for ERA5 profiles on 18 June 2018.

Humid air is lighter than dry air. This is considered in the calculation of  $V_{O_4, \text{true}}$ . For  $V_{O_4, \Gamma}$ , however, dry air is assumed in the derivation in section 2. One would thus expect that the observed deviation is affected by humidity. However, when comparing to specific humidity at surface, we found no correlation (Fig. ?? (a)). We also compared to the total column of water vapor (TCWV), i. e. the vertically integrated water vapor number density. The reason for choosing this quantity was that it (a) represents the total amount of water vapor rather than just the surface value and (

In Fig. 5 (a), the effective lapse rate is compared to the actual lapse rate between ground and 5 km altitude above ground, revealing a correlation of 0.83. Figure 5 (b) could also be derived from MAX-DOAS measurements directly. But again, we found no correlation (displays the relation between relative humidity at ground and the effective lapse rate ( $R=0.59$ )). Assuming a linear relation between  $\Gamma_{\text{eff}}$  and  $RH_0$  in Eq. 13 results in a linear relation between  $RH_0$  and the ratio  $Q$  (Eq. 18). This is displayed in Fig. ?? (b)).

Instead, we observed a very good correlation between relative humidity and (Fig. ?? (5 (c)). Interestingly, the correlation ( $R=0.79$ ) is far better than in (b) ( $R=0.59$ ). This cannot be explained by the impact of humidity on air density, as this is a direct function of specific humidity. But RH at surface is closely related to the effective lapse rate: for ascending air, RH indicates



**Figure 5.** Relations between lapse rate,  $\text{RH}_0$  and ratio  $Q$  for ERA5 data on 18 June 2018. (a) Relation between the actual lapse rate (calculated from the temperature difference between ground and 5 km altitude) and the effective lapse rate. (b) Relation between  $\text{RH}_0$  and effective lapse rate. (c) Relation between  $\text{RH}_0$  and the ratio  $Q$  as defined in Eq. 18, where the black line shows the linear fit  $a + b \cdot \text{RH}_0$ .

335 that the parameterization based on  $\text{RH}_0$  determines the lifted condensation level (LCL) (Lawrence, 2005; Romps, 2017): the lower  $\text{RH}_0$ , the higher the LCL, with dry-adiabatic lapse rates below. For tropical deserts, on the other hand, which are affected by large-scale subsidence, no condensation takes place (allows to at least partly correct for other simplifications made in the formalism in Sect. 2.3, in particular the neglect of humidity in the ideal gas law).

We use ERA5 data from 18 June 2018 to determine the parameters  $a$  and  $b$  in Eq. 14 by applying a linear least squares fit to the data presented in Fig. 5 (c), as shown by the black line. Fitted parameters are  $a = 1.77434 \pm 0.00003$  and  $b = 0.11821 \pm 0.00004$  (for  $\text{RH}_0$  in absolute numbers, i.e. the dry-adiabatic lapse rate applies), and  $\text{RH}_0$  at ground is very low due to the adiabatic heating of the descending air masses. Thus, the main systematic deviations seen in are caused by the simple assumption of a constant lapse rate of  $-6.5$  to  $-0.5$  for 50% RH. The corresponding parameterisation of the effective lapse rate (Eq. 13) is  $\Gamma_{\text{eff}} = (-7.709 + 4.038 \cdot \text{RH}_0)$  K km<sup>-1</sup>, while actual effective lapse rates are far stronger (more negative) over deserts, with low which yields  $-7.709$ ,  $-5.690$  and  $-3.671$  K km<sup>-1</sup> for  $\text{RH}_0 = 0\%$ ,  $50\%$  and  $100\%$ , respectively. Over most parts of the ocean, on the other hand,  $\text{RH}_0$  is high, and the effective lapse rate is weaker (closer to zero).

Deviation according to eq. ?? as function of (a) specific humidity at surface, (b) total column water vapor, and (c) relative humidity at surface for ECMWF data on 18 June 2018, 12:00 UTC. Only 1% of the data points are plotted in order to keep the figure readable. Correlation coefficients are given in the respective subplots.

350 We make use of the good correlation of  $\Gamma_{\text{eff}}$  to  $\text{RH}_0$  in order to construct an empirical parameterization according to eq. 20. For this purpose, the parameters  $a$  of 0%, 50%, and  $b$  were determined by a linear least squares fit (after re-arranging eq. ?? for  $a + b \cdot \text{RH}_0$ ) to global ECMWF data for 18 June 2018. 100%, respectively.

### 4.3 O<sub>4</sub> VCD as function of p<sub>0</sub>, T<sub>0</sub>, and RH<sub>0</sub>

With [eq. 14](#), an empirical parameterization of the O<sub>4</sub> VCD was derived based on surface values of temperature, pressure, and relative humidity. We applied this parameterization to all investigated datasets. Figures [??](#), [??](#) and [??](#) [6](#) and [7](#) display  $\delta_{RH}$  for WRF and [ECMWF-ERA5](#), respectively. GRUAN results are [listed in table ??](#) shown in [Fig. 8](#).

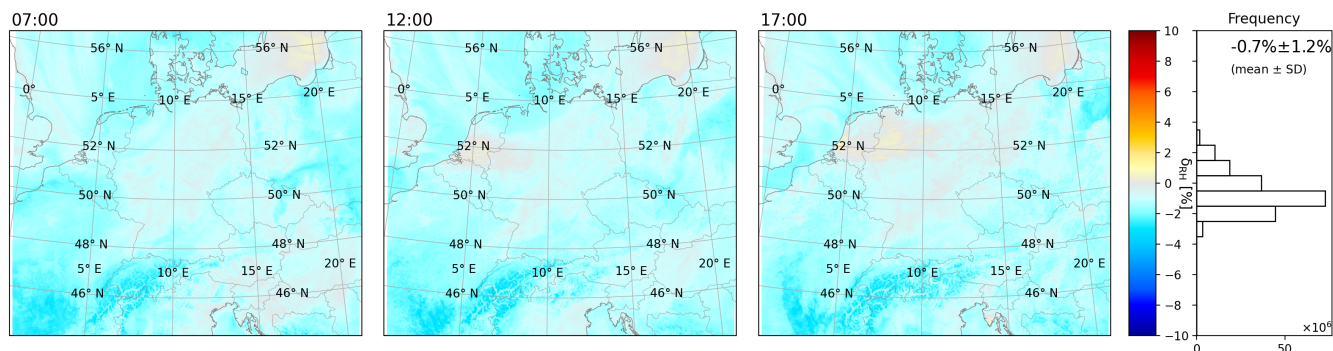


**Figure 6.** Deviation  $\delta_{RH}$  according to [eq. 19](#) for WRF simulations at 7:00, 12:00, and 17:00 UTC on 1 May 2018. On the right, the frequency distribution and mean and SD are given for the WRF simulation period from [1 to 9 May 2018](#).

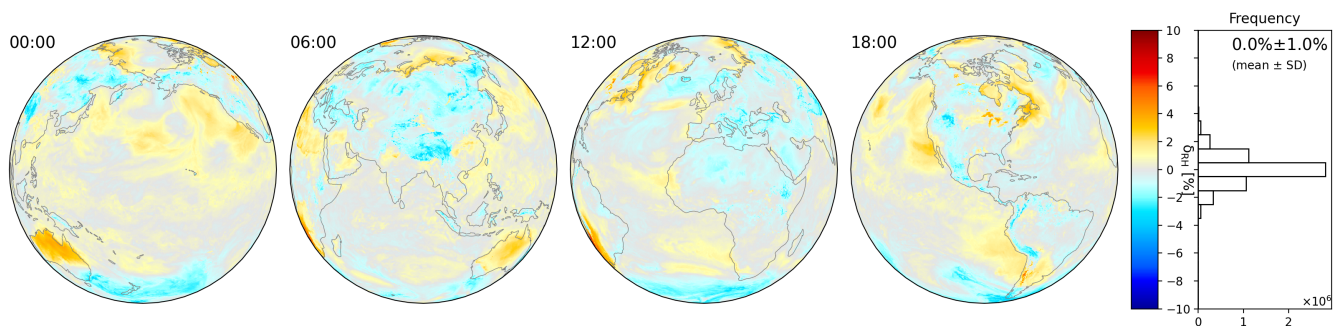


**Figure 7.** Deviation  $\delta_{RH}$  according to [eq. 19](#) for [ECMWF-ERA5](#) at 0:00, 6:00, 12:00 and 18:00 UTC on 18 June 2018. The projection focuses on daytime for each timestep. On the right, the frequency distribution and mean and SD are given for all hourly outputs from 18 June 2018. Respective deviations for days in other seasons are shown in [Fig. C2](#).

**Deviation according to eq. ?? for ECMWF at 0:00, 6:00, 12:00 and 18:00 UTC on 18 December 2018. The projection focuses on daytime for each timestep. On the right, the frequency distribution and mean and SD are given for all hourly outputs from 18 December.**

For the WRF [domain-d02 simulations](#),  $\delta_{\Gamma}$  was already quite close to 0 (mean  $\delta_{\Gamma} = -1.5\% = -1.6\%$ , see [Fig. 2](#)).  $\delta_{RH}$  ([Fig. 6](#)) is closer to 0, but now showing a slight negative bias (mean  $\delta_{RH} = -0.9\% = -0.7\%$ ). Variability has reduced considerably (SD

of  $\delta_{RH}$  is ~~1.0%~~1.2%, compared to ~~1.6%~~1.9% for  $\delta_{\Gamma}$ .  $\delta_{RH}$  shows a weaker land-ocean contrast. Over the Alps,  $\delta_{RH}$  is biased low (down to  $-3\%$ ).

For ~~ECMWF ERA5~~, the parameterization involving RH is a substantial improvement compared to the results for  $\delta_{\Gamma}$ . The large difference between land (in particular deserts) and oceans seen in  $\delta_{\Gamma}$  (Fig. 3) is strongly reduced for  $\delta_{RH}$  (Fig. 7). For 18  
365 June 2018, the mean of  $\delta_{RH} = 0.0\% \equiv 0.0\%$  is of course a consequence of the fit optimizing  $a$  and  $b$  which is based on the same ~~ECMWF ERA5~~ dataset. But there is also a considerable reduction of SD from 1.6% for  $\delta_{\Gamma}$  to 1.0% for  $\delta_{RH}$ . ~~Land-ocean contrasts are suppressed, but are still visible for some coastlines like the West coasts of North and South America. The low values over deserts observed for are largely improved for.~~ Applying Eq. 14, with  $a$  and  $b$  derived from ERA5 data for 18 June 2018, to ECWFM data from other months yields similar results, as shown in Fig. C2, with largest deviations of  $0.2 \pm 1.8\%$  observed for 18 March 2018.

~~For December, mean (based on the parameterization optimized for June) is close to 0 as well (0.1%). SD improved slightly (SD = 1.3% for vs. 1.2% for).~~

Remaining systematic deviations in the maps of  $\delta_{RH}$  are ~~basically~~ due to

- weather, for instance associated with low pressure or frontal systems. This reflects the simplifying assumptions made, in particular assuming hydrostatic conditions in ~~section Sect. 2~~. Note, however, that MAX-DOAS retrievals are usually not considered for weather conditions associated with rain and clouds ~~are usually not considered in MAX-DOAS retrievals.~~
- cold surfaces causing temperature inversions, as discussed in more detail in Sect. 5.2.
- mountains, which tend to show systematic deviations  $\delta_{RH}$  that are mostly negative (e.g. over the Andes ~~), but sometimes also positive (e. g. over Antartica) or the Himalayas~~). For further discussion see ~~sect. ??~~ Sect. 5.4.
- some patterns of enhanced  $\delta_{RH}$  at the Northern, Southern, or Western edge of the maps for ~~ECMWF ERA5~~, corresponding to high solar zenith angles: polar regions as well as sampling times shortly after sunrise (e.g. over South Africa at 6:00 UTC).

So far, the formalism derived in ~~section Sect. 2~~ was applied to data from ~~meteorological~~ meteorological models. Now we test it for ~~radiosonde profiles measured profiles from radiosondes~~ as well. Application of ~~eq-20~~ Eq. 14 to GRUAN data ~~yields low deviations generally yields deviations close to 0~~ between parameterized and true  $O_4$  VCDs ~~close to 0~~ for all stations, as ~~listed in table ??~~. Overall, the shown in Fig. 8. Parameterized and true VCD show high correlations, indicating that the temporal variability of the atmospheric state is well captured by the simple parameterization based on surface values alone. The mean deviation  $\delta_{RH}$  of all considered GRUAN profiles is  ~~$-0.4\%$~~  $-0.3\%$ , with a SD of 1.4%. For 11 out of the 17 stations, the mean agreement is within 1%.

390 Largest deviations are found for La Reunion (REU), where  $V_{O_4, RH}$  is biased low by  $-2.5\%$ . This is probably related to the altitude of this station of more than 2 km on a remote island in the Indian ocean.

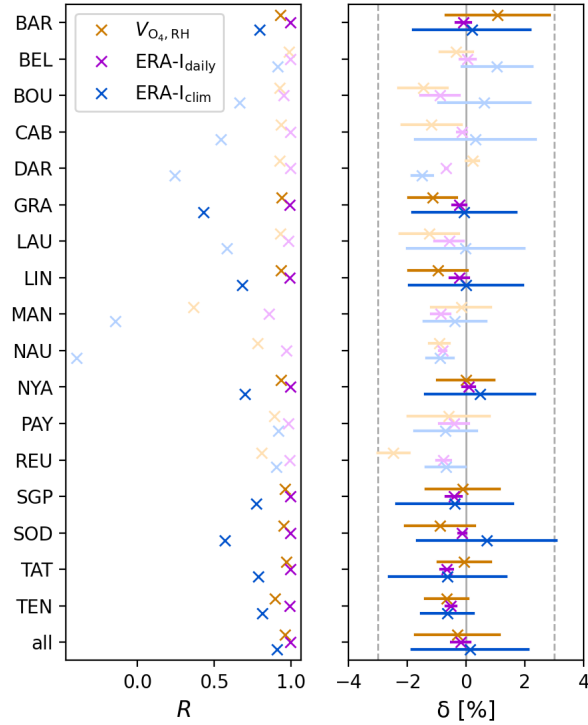


**Figure 8.** Deviations for GRUAN stations. Additional information on GRUAN stations is given in Appendix B1. In Comparison to the last column, also the true  $O_4$  VCD in terms of temporal correlation coefficient (top) and deviation  $\delta_{ECMWF, \delta}$  according to Eq. e: the relative difference between integrated-19 (bottom) for all GRUAN stations for  $O_4$  VCDs calculated from (a) Eq. 14 based on ECMWF-GRUAN surface values (orange), (b) daily ERA-Interim profiles (interpolated in space and time to the radiosonde data purple) and GRUAN (c) profiles is shown. The last row from the ERA-Interim climatology (all blue) is, interpolated to the mean of all available profiles GRUAN measurements in space and is thus reflecting conditions of the time. Light colors indicate stations with high number of radiosonde measurements less than 100 profiles (compare Table B1).

Station  $\delta_{RH} \%$   $\delta_{ECMWF} \%$  Barrow  $1.0 \pm 1.8$   $-0.1 \pm 4.8$  Beltsville  $-0.3 \pm 0.5$   $-0.6 \pm 2.5$  Boulder  $-1.4 \pm 0.8$   $-9.5 \pm 2.7$  Cabauw  $-1.2 \pm 1.0$   $-0.3 \pm 3.9$  Darwin  $0.3 \pm 0.2$   $-0.8 \pm 0.6$  Graciosa  $-1.2 \pm 0.8$   $-0.6 \pm 3.5$  Lauder  $-1.3 \pm 1.0$   $-6.9 \pm 3.0$  Lindenberg  $-1.0 \pm 1.0$   $-0.6 \pm 3.7$  Manus  $-0.2 \pm 1.1$   $-1.1 \pm 0.8$  Nauru  $-0.9 \pm 0.3$   $-1.0 \pm 0.5$  NyAlesund  $-0.0 \pm 1.0$   $-3.5 \pm 3.2$  Payerne  $-0.7 \pm 1.4$   $-10.0 \pm 2.8$  LaReunion  $-2.5 \pm 0.5$   $-3.4 \pm 5.6$  Lamont  $-0.1 \pm 1.3$   $-1.2 \pm 4.3$  Sodankyla  $-0.9 \pm 1.2$   $-1.3 \pm 4.4$  Tateno  $-0.1 \pm 0.9$   $-2.5 \pm 3.9$  Tenerife  $-0.6 \pm 0.7$   $-0.5 \pm 2.7$  all  $-0.4 \pm 1.4$   $-1.2 \pm 4.2$

Highest positive deviation of  $1.0\%$   $1.1\%$  is found for Barrow, with also highest SD of 1.8%. Closer inspection revealed that for Barrow, the high SD is mainly This is caused by some very high values during spring where surface temperatures are very low ( $< 240$  K) and temperature inversions occur (i. e. lapse rates are positive in the boundary layer).

### 5.1 Accuracy and precision

In eq. 20, we provide a formula for the ~~Comparison to existing methods for the~~ calculation of the  $O_4$  VCD. ~~Accuracy and precision of the resulting  $V_{O_4}$  thereby depend on accuracy and precision of~~ ( Within MAPA (Beirle et al., 2019), the  $O_4$  VCD was so far determined by integrating vertical profiles of the  $O_4$  number density based on full profiles of  $T$ ,  $p$  and RH, which are by default taken from daily ERA-Interim simulations (ERA-I<sub>daily</sub>), or, as fallback solution, from a monthly climatology compiled from multi-annual ERA-Interim data (ERA-I<sub>clim</sub>), both on  $1^\circ$  resolution.

Thus, we evaluate the performance of the proposed simple calculation of the ~~chosen parameterization and~~ ( $O_4$  VCD by comparing the results for GRUAN profiles, where the true  $O_4$  VCD is known, also to the ERA-Interim profiles interpolated in space and time. In addition, a correction of surface altitude is necessary: For La Reunion, for instance, the radio sondes launched at a surface altitude of  $2$  ~~surface values  $p_0$~~ , km, while the surface altitude in ERA-Interim (with  $1^\circ$  resolution) is just 54 m. This could easily cause deviations of 10% in  $O_4$  VCDs when ignored. Thus we apply the following correction to the ERA-Interim profiles:

- In case of GRUAN station altitude being higher than ERA-Interim surface altitude, the ERA-Interim profiles of  $T$  and RH are just linearly interpolated. As pressure profiles are almost exponential,  $\ln(p)$  is linearly interpolated.
- In case of GRUAN station altitude being lower than ERA-Interim surface altitude, ERA-Interim profiles are extended by surface values of  $T_0$  and  $RH \ln(p_0)$  as derived from linear extrapolation of  $T$  and  $\ln(p)$ , respectively. RH at ground, however, is not extrapolated, as this might result in unphysical values of RH below 0 or above 1. Instead, the value of the lowest ERA-Interim model layer is taken as  $RH_0$ .
- We estimate overall accuracy and precision of eq. 20 to  $< 1\%$  and  $< 2\%$  based on

We calculate the deviation to the true VCD (defined by the GRUAN profiles) according to Eq. 19 for daily and climatological ERA-Interim data. The correlation coefficients as well as mean and SD of ~~deviations between parameterized and true the~~ resulting deviations are also included in Fig. 8.

For  $O_4$  VCD for WRF, ECMWF and GRUAN data as presented above. For high SZA as well as for mountaineous regions (see also section ??), uncertainties can be larger up to about 3%. Application of eq. 20 requires surface measurements of  $p_0$ ,  $T_0$  VCDs based on daily ERA-Interim profiles, the agreement to VCDs integrated from GRUAN profiles is generally very good. Correlation coefficients are almost 1 and deviations are close to 0 for most stations. Only for mountainous sites as Boulder, where surface altitude differ between GRUAN and ERA-Interim, clear deviations from 0 are found.

Results based on the ERA-Interim climatology, however, show far weaker correlation than for daily ERA-Interim data, as they do not resolve day-to-day changes in meteorology. Mean deviations are within  $\pm 1\%$  for most stations, with a SD of about 2%.

In comparison to these existing methods, the  $O_4$  VCDs based on Eq. 14 are worse than those based on daily ERA-Interim profiles, but significantly better than those based on a profile climatology, in particular in terms of correlation and SD.

## 5.2 Impact of temperature inversions

430 The presented parameterizations derive the  $O_4$  VCD just from surface values of  $T$ ,  $p$ , and  $RH_0$ . Uncertainties of temperature and pressure are rather uncritical, as an error of 1 K and 1 hPa for  $T_0$  and  $p_0$  would correspond to an error of 0.3% and 0.2% in  $V_{O_4, RH}$ , respectively. In order to reach an accuracy/precision of 1%, the corresponding errors of  $RH_0$  have to be lower than 16%. These limits should be achievable for adequate meteorological instrumentation and a measurement procedure following WMO guidelines. In particular, surface temperature should be measured at about 1.25–2 m above ground using a radiation shield (WMO, 2018). This requires some basic assumptions about the atmospheric profile shape. In case of temperature  
435 inversions, these assumptions do not hold. Thus, we focused on daytime conditions by selecting only data with  $SZA < 85^\circ$ . But still, temperature inversions can also occur during daytime, in particular over cold water and ice surfaces, as well as shortly after sunrise.

The proposed parameterization thus allows to calculate VCD with accuracy and precision sufficient for applications in Figure 9 displays temperature inversions, here defined as the difference between tropospheric maximum and surface temperature, for  
440 ERA5 data on 18 June 2018. Strong temperature inversions are found e.g. over Hudson Bay or the Great lakes where sea surface temperature is low. Also at the Western edge of the illuminated Earth (i.e. shortly after sunrise), temperature inversions occur, e.g. in North and South Africa at 6:00 UTC, indicating remainings of nocturnal profiles.

Large parts of the regions with high positive deviation  $\delta_\Gamma$  (Fig. 3) or  $\delta_{RH}$  (Fig. 7) actually correspond to temperature inversions. Thus, for MAX-DOAS profile inversions. Interestingly, the default procedure used in MAPA, i. e. integrating the  
445 measurements close to cold surface waters or other regions with temperature inversions, the formalism of Eq. 10 and Eq. 14 should only cautiously be applied, and corrections of surface temperature might be needed for better results. For the discussion below, temperature inversions of more than 2 K have been skipped from ERA5 data in order to avoid interference of different effects, in particular over Antarctica.

## 5.3 Impact of humidity

450 The formalism in Sect. 2.3 is assuming dry air. Addition of humidity results in lower  $O_2$  and  $O_4$  VCD based on ERA-Interim profiles pre-gridded on  $1^\circ$  resolution, results in larger deviations (in particular larger SD) when applied to GRUAN profiles (see table ??). We thus consider the proposed parameterization as useful approach for determining the number densities, which significantly affects the  $O_4$  VCD, especially in the tropics (Wagner et al., 2019). Humidity affects all terms in Eq. 6 (i.e. the  $O_2$  VCD, the  $O_2$  surface number density, and the ratio of effective heights of  $O_2$  and  $O_4$ ), but cannot be accounted for in the  
455 formalism without completely losing the simplicity of Eq. 10.

However, these effects are partly accounted for in Eq. 14, with empirically determined parameters  $a$  and  $b$ , since the ratio  $Q$  was determined based on the true  $O_4$  VCD where humidity effects were appropriately accounted for.

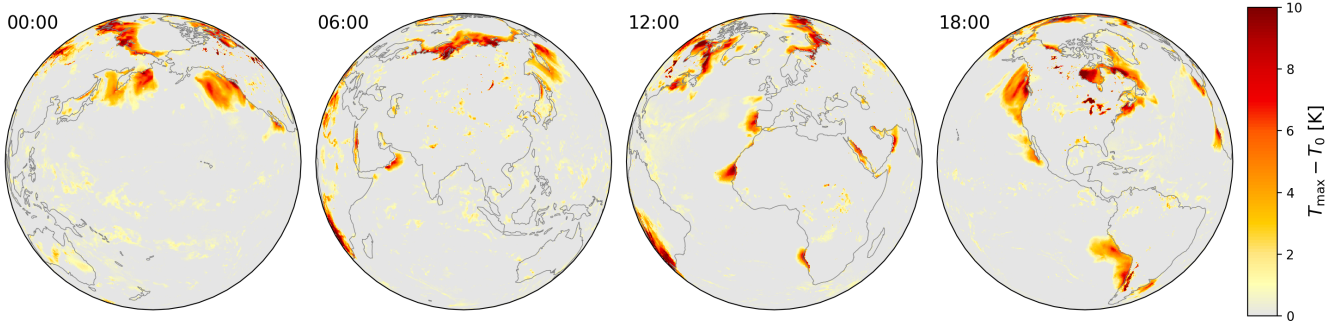


**Figure 9.** Temperature inversions, expressed as difference between tropospheric maximum and surface temperature, for ERA5 simulations at 0:00, 6:00, 12:00, and 18:00 UTC on 18 June 2018.

460 In order to check for possible remaining impacts of humidity on the performance of Eq. 14, we check how far  $\delta_{RH}$  is related to specific humidity at ground (Fig. 10). In addition, we compare  $\delta_{RH}$  also to the total column water vapor, as this provides information on humidity in the full column, not only at surface. In both cases, correlations are low, and no significant impact of humidity on  $\delta_{RH}$  could be found.

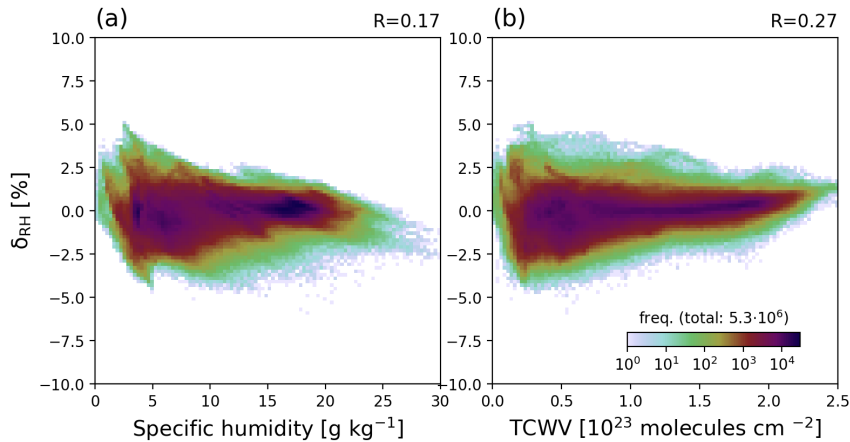


**Figure 10.** Deviation  $\delta_{RH}$  according to Eq. 19 as function of (a) specific humidity at ground, and (b) TCWV for ERA5 simulations on 18 June 2018. Temperature inversions with  $T_{max} - T_0 > 2$  K have been skipped.

#### 5.4 Impact of surface altitude

Figures 6 and 7 reveal systematic spatial patterns in  $\delta_{RH}$  corresponding to mountains. We thus investigate a possible relation between surface altitude and  $\delta_{RH}$  for all investigated datasets (Fig. 11).

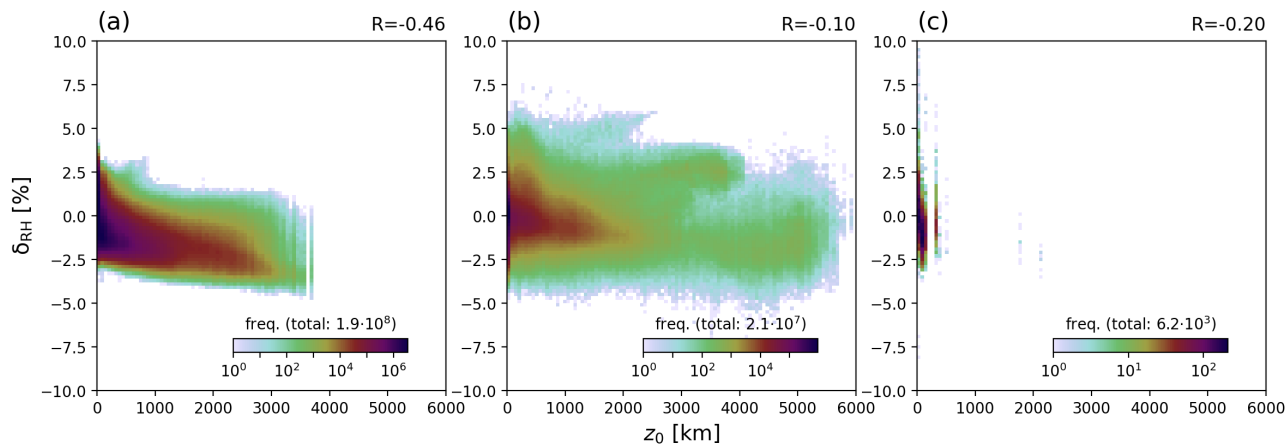


**Figure 11.** Dependency of  $\delta_{RH}$  on surface altitude for (a) WRF data for May to June 2018, (b) ERA5 data for all selected days, and (c) GRUAN data. For (b), Temperature inversions with  $T_{max} - T_0 > 2$  K have been skipped.

465 For the WRF simulations, the Alps can be clearly recognized in Fig. 6, with mountains showing lower values of  $\delta_{RH}$ . This can also be seen in the density plot in Fig. 11 (a), where surface altitude and  $\delta_{RH}$  are anticorrelated with  $R = -0.46$ , and a decrease of  $\delta_{RH}$  of roughly 1 % per km. For GRUAN stations (c), results are similar, but statistics are poor, and the correlation coefficient is low, as only two stations (Boulder and La Reunion) are available with a surface altitude above 1 km.

470 For ERA5, however, results are not as clear as those for WRF. The correlation coefficient is low, and for altitudes between 2 and 3 km, it looks like  $\delta_{RH}$  is increasing rather than decreasing with altitude. And for very high surface altitudes as found over the Himalaya,  $\delta_{RH}$  is still close to 0 and would not match the slope of 1 % per km estimated for WRF.

475 The reason for the poor correlation between  $z_0$  and  $\delta_{RH}$  for ERA5 compared to the WRF results is not clear to us. Obviously, other factors would probably also have to be considered (season, SZA). But since there is no clear correlation, and a quantitative correction would rather worsen  $\delta_{RH}$  instead of improving it for several mountain areas around the globe, we decided not to apply an explicit correction for surface altitude.

Consequently, the parameterization of Eq. 14 has higher uncertainties when applied for mountainous sites: for  $z_0 > 2$  km,  $\delta_{RH}$  is  $-0.5\%$  on average with a SD of  $1.8\%$ . But still, the parameterized  $O_4$  VCD even for cases where model profiles are available matches the requirement of accuracy/precision better than 3 % even for elevated sites.

## 5.5 Diurnal cycles

480 Surface conditions can change rapidly, e.g. in case of passing frontal systems or storm tracks. For such rapid changes, the change of the true  $O_4$  VCD might not be adequately represented by the change of  $V_{O_4, RH}$ . These effects are reflected in the SD of deviations  $\delta_{RH}$  for ECMWF/ERA5, WRF, and GRUAN.

In addition, surface values could change *systematically* during the day in case of strong solar irradiation, causing a diurnal cycle of surface temperature and the  $O_4$  VCD (Wagner et al., 2019). Thus we investigate the diurnal cycles of  $T_0$ ,  $p_0$ ,  $RH_0$ , and

485 the respective  $O_4$  VCDs  $V_{O_4, RH}$  and  $V_{O_4, true}$  in more detail, and [investigate-check](#) how far (a) the WRF simulations reflect the actual diurnal cycles and (b) the parameterized  $O_4$  VCD based on surface values reflect the diurnal cycle of the true  $O_4$  VCD. For this, we extract the WRF simulations at the locations of the DWD ground station network. In order to focus on strong diurnal patterns, we select [at each station those](#) days where the change of surface temperature, [as recorded by DWD](#), exceeds 10 K [for each station](#).

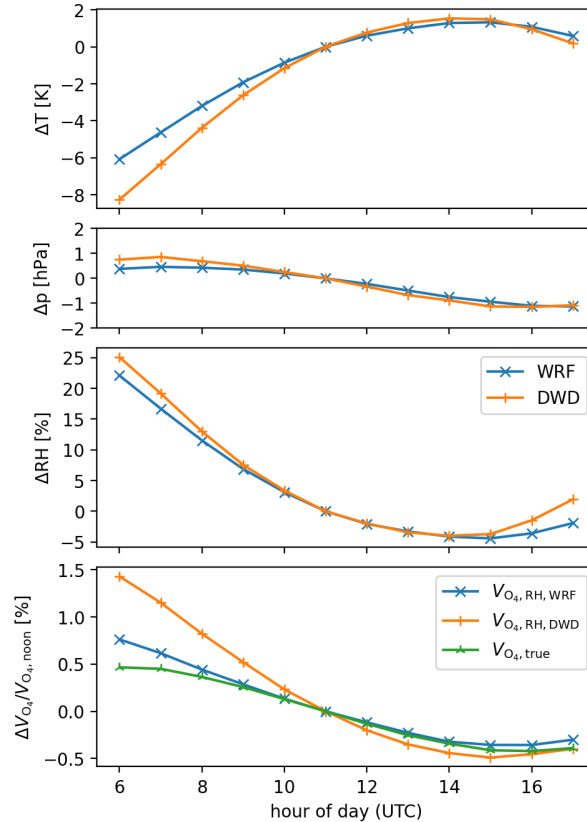


**Figure 12.** Diurnal cycles of surface temperature (a), pressure (b), RH (c), and the  $O_4$  VCD (d). Data points show the mean values for all stations for [the considered time period 1-9 May to June 2018](#) for days where [the increase in  \$T\_0\$  \(from DWD\) over the day is larger than 10 K](#). For better comparison, [all cycles are referred to the mean value at 11:00 UTC \(around solar noon for Germany\) is subtracted from all datasets](#). For the  $O_4$  VCD, the relative change is shown.

490 [Fig. ?? Figure 12](#) displays the diurnal cycles of surface properties and  $O_4$  VCDs for WRF and DWD station data. [Overall, the diurnal cycle simulated by WRF matches the patterns measured by the surface stations quite well, and  \$V\_{O\_4, RH}\$  is almost the same for WRF and ground stations. Surface pressure changes only slightly over the day; the systematic decrease is of the same magnitude as the respective standard mean error for each hour of the day of about 2.5 hPa. But \[While surface pressure shows no relevant changes during day\]\(#\), surface temperature increases by \[10.5 K-9.8 K\]\(#\) from morning to \[evening-afternoon\]\(#\) due](#)

495 to the selection of days with strong diurnal cycle in  $T_0$ -surface temperature<sup>2</sup>. For WRF simulations, a similar pattern is found,  
but the mean temperature increase over the day is smaller (7.4 K). As  $V_{O_4, RH}$  is reciprocal to  $T$ , this  $T_0$ , a change of 10 K  
in surface temperature alone would correspond to a change of  $V_{O_4, RH}$  of 3.5%. However, at the same time, RH decreases by  
about 30%, which has an opposite effect on  $V_{O_4, RH}$ . Consequently, the diurnal cycle of  $V_{O_4, RH}$  is only moderate (about 2%  
1.9% and 1.1% decrease from morning to evening for DWD and WRF, respectively, where the cycle for WRF is less strong  
500 due to the less strong cycle in  $T_0$ ).

The true  $O_4$  VCD, as derived from the integrated WRF profiles, also decreases over the day, and  $V_{O_4, true}$  follows nicely  
 $V_{O_4, RH}$  agrees well to  $V_{O_4, RH}$  (WRF) in the afternoon. In the morning, however,  $V_{O_4, RH}$  (WRF) is higher compared to noon  
by 1.4%–0.8%, while  $V_{O_4, true}$  is only 0.7%–0.5% higher. This deviation between parameterized and true  $O_4$  VCD indicates  
that in the early morning, surface measurements are not as useful for determining the full column, which is probably related to  
505 remainders of the nocturnal boundary layer which often has atypical lapse rates due to temperature inversions.

But even during morning hours, the systematic error made by  $V_{O_4, RH}$  is relatively small, at least for the investigated time  
period for Germany. But also for the global ECMWF-ERA5 analysis, the impact of diurnal cycles on the calculation of the  $O_4$   
VCD is only moderate; otherwise, Figures ?? and ??-7 and C2 would show systematic East-West gradients.

Thus, the parameterization of eq-20 also reflects Eq. 14 also reflects most of the diurnal cycle of the  $O_4$  VCD sufficiently,  
510 with remaining systematic errors below 0.3%.

## 5.6 Dependency on surface altitude

### 5.6 Accuracy and precision

In Eq. 14, we provide a formula for the calculation of the  $O_4$  VCD. Accuracy and precision of the resulting  $V_{O_4}$  thereby depend  
on accuracy and precision of (1) the chosen parameterization and (2) surface values  $p_0$ ,  $T_0$  and  $RH_0$ .

515 The empirical parameterization eq-20 works generally well, but is of course not perfect. Remaining patterns in the maps of  
show weather patterns like low pressure systems, but also some systematic effects. In particular mountains can be recognized  
in Figures ??, ?? and ?? We thus investigate a possible relation between surface altitude and for all investigated datasets  
(Fig. ??).

Dependency of on surface altitude for (a) WRF, (b) ECMWF, and (c) GRUAN data. For (a) and (b), only 0.2% of the data  
520 points are plotted in order to keep the figure readable.

For the WRF simulations for the domain d02, the Alps can be clearly recognized in Fig. ??, with mountains showing lower  
values of . This can also be clearly seen in the scatter plot in Fig. ?? (a), where surface altitude and are anticorrelated with  
 $R = -0.53$ , and a decrease of of roughly 1% per . For GRUAN stations (c), results are similar, but statistics are poor, and the  
correlation coefficient is low, as only two stations (Boulder and La Reunion) are available with a surface altitude above 1 km

---

<sup>2</sup> Note that the mean change is lower than the threshold used for the selection of DWD stations. This is caused by averaging diurnal cycles with maxima  
occurring at different times of the day.

525 1. We estimate overall accuracy and precision of Eq. 14 to < 1% and < 2% based on mean and SD of deviations between parameterized and true O<sub>4</sub> VCD for WRF, ERA5 and GRUAN data as presented above. Higher deviations can occur in particular in case of temperature inversions (see Sect. 5.2).

For ECMWF, however, results are not at all as clear as those for WRF. The correlation coefficient is close to zero. For altitudes between 2 and 3 km, it looks like  $\gamma$  is increasing rather than decreasing with altitude. And for very high surface altitudes as found over the Himalaya,  $\gamma$  is still close to 0 and would not match the slope of 1% per derived for WRF. Especially for 18 December 2018, it can clearly be seen that the impact of surface altitude is ambiguous (Fig. ??): While deviations over the Andes are strongly negative, they are positive over the Himalayas as well as over Antarctica. The reason for the poor correlation between  $\gamma$  and  $z_0$

530 2. Application of Eq. 14 requires surface measurements of  $p_0$ ,  $T_0$ , and  $RH_0$ . Uncertainties of temperature and pressure are rather uncritical, as an error of 1 K and for ECMWF is not clear to us. Obviously, also other factors would probably have to be considered (season, SZA). But since there is no clear correlation, and a quantitative correction would rather worsen instead of improving it for several mountain areas around the globe, we decided not to apply an explicit correction for surface altitude.

Consequently, the parameterization of eq. 20 has higher uncertainties up to about 3% when applied for mountainous sites.

## 5.7 Application for MAX-DOAS profile inversions based on optimal estimation

For profile inversion schemes based on profile parameterizations, like MAPA (Beirle et al., 2019), the VCD is needed in order to convert the measured SCDs to AMFs. For inversion schemes based on optimal estimation, however, vertical profiles of  $T$  1 hPa for  $T_0$  and  $p$  are required for the online RTM calculations. For this case, we propose to extrapolate profiles of  $T$  and  $p$  from surface values as proposed in Wagner et al. (2019), but not with a constant lapse rate. Instead, the effective lapse rate should be determined from surface RH according to equations ?? and ??:

$$2 + \frac{R}{g \cdot M} \Gamma = a + b \cdot RH_0$$

and thus

$$\Gamma = (a - 2 + b \cdot RH_0) \cdot \frac{g \cdot M}{R}$$
$$= (-0.2308 + 0.1257 \cdot RH_0) \cdot 34.16 \text{ K km}^{-1}$$

550 For  $RH_0$  would correspond to an error of 0.3% and 0.2% in  $V_{O_4, RH}$ , respectively. In order to reach an accuracy/precision of 1%, the corresponding errors of  $RH_0$  of 0%, 50%, and 100%, the corresponding effective lapse rate results in  $-7.89$ ,  $-5.74$ , and  $-3.59 \text{ K km}^{-1}$ , respectively. These limits should be achievable for

adequate meteorological instrumentation and a measurement procedure following WMO guidelines. In particular, surface temperature should be measured at about 1.25 to 2 m above ground using a radiation shield (WMO, 2018).

## 555 5.7 ~~Lapse rate from direct sun measurements of and~~

~~Eq. 6 relates the~~ The proposed parameterization thus allows to calculate  $O_4$  VCD to the ratio of effective heights for and, which can be expressed by the effective atmospheric lapse rate (see Appendix A). This formalism might also be used in the other direction: ~~from total column measurements of and by direct sun observations,~~ an effective atmospheric lapse rate can be derived:-

$$560 \quad 2 + \frac{R}{g \cdot M} \cdot \Gamma = \frac{h_{O_2}}{h_{O_4}} = \frac{V_{O_2}}{V_{O_4}} \cdot n_{O_2,0} = \frac{S_{O_2}}{S_{O_4}} \cdot \frac{\nu_{O_2} \cdot p_0}{R \cdot T_0}$$

~~and thus~~

$$\Gamma = \left( \frac{S_{O_2}}{S_{O_4}} \cdot \frac{\nu_{O_2} \cdot p_0}{R \cdot T_0} - 2 \right) \cdot \frac{g \cdot M}{R}$$

~~with  $S$  being the slant column of the direct sun measurement. For direct sun measurements, the ratio between slant and vertical column is a simple function of the SZA and is the same for and~~ VCD with overall uncertainties below 3%, which is   
 565 sufficient for applications in MAX-DOAS profile inversions. Compared to existing methods, the parameterization yields even better results than a profile climatology.

~~Even for limited accuracy of column measurements of and~~ We thus consider the proposed parameterization as useful approach for determining the  $O_4$ , ~~this would allow to derive time series of an effective lapse rate, reflecting the state of the lower atmosphere~~ VCD for cases where no daily model profiles are available, and recommend to also apply it for mountain   
 570 sites for comparison and possible correction of daily model profiles.

## 6 Conclusions

The  $O_4$  VCD can be expressed in terms of surface pressure and temperature based on physical laws, if a constant lapse rate is assumed, without the need for constructing full vertical profiles. With an empirical correction which ~~basically~~ parameterizes the effective lapse rate as linear function of surface RH, we could present a formula for simple and quick calculation of the  $O_4$    
 575 VCD based on  $p_0$ ,  $T_0$ , and  $RH_0$ :

$$V_{O_4, RH} = \frac{6.733 \cdot 10^{39}}{1.774 + 0.1182 \cdot RH_0} \cdot \frac{p_0^2}{T_0} \text{ molec}^2 \text{ cm}^{-5}. \quad (20)$$

This parameterization reproduces the real  $O_4$  VCD, as derived from vertically integrated profiles, within  ~~$-0.9\% \pm 1.0\%$~~   $-0.7\% \pm 1.2\%$  for WRF simulations around Germany,  ~~$0.1\% \pm 1.2\%$~~   $0.2\% \pm 1.8\%$  for global reanalysis data (ERA5), and  ~~$-0.4\% \pm 1.4\%$~~   $-0.3\% \pm 1.4\%$  for radiosonde soundings around the world. ~~Uncertainties over mountains are generally larger~~

580 ~~(up to about 3%)~~ Largest deviations are observed in case of temperature inversions which cause too low  $T_0$  (compared to the remaining profile) and thus high biased estimates of  $V_{O_4, RH}$ . For applications to measured surface values, uncertainties of 1 K, 1 hPa, and 16 % for temperature, pressure, and RH correspond to relative uncertainties of the  $O_4$  VCD of 0.3 %, 0.2 %, and 1 %, respectively.

This accuracy and precision ~~is sufficient~~ of  $< 3\%$  is typically lower than other uncertainties of spectral analysis or radiative transfer modeling (Wagner et al., 2019). Thus, the proposed parameterization is well suited for application in MAX-DOAS profile inversions. Moreover, the parameterization reflects the true  $O_4$  VCD, as derived from radiosonde measurements, even better (in particular in terms of temporal correlation and SD) than ~~the standard approach we used so far for MAPA based on interpolated model data~~  $O_4$  VCD calculated from a climatology of atmospheric profiles of  $T$ ,  $p$  and RH. We thus recommend to equip ~~each~~ MAX-DOAS measurement ~~station~~ stations with state-of-the-art thermometer (with radiation shield), barometer, 590 and hygrometer.

*Code availability.* A Python implementation of the derived functions for the calculation of the  $O_4$  VCD is provided in the Supplementary material.

## Appendix A: Ratio of effective heights

The ratio of the effective heights for ~~and~~  $O_4$  and  $O_2$  in Eq. 6 depends on the shape of the  $O_2$  profile. For specific shapes  
595 the ratio can be calculated explicitly. ~~Here, vertical integration is performed to infinity.~~ Below, we derive the ratio  $\frac{h_{O_2}}{h_{O_4}}$ , which  
allows for simpler notation avoiding compound fractions. For application in eqEq. 6, the inverse ratio has to be taken.

### A1 Isothermal atmosphere

For the simple assumption of a barometric pressure profile with constant  $T$ , the  $O_2$  number density decreases exponentially  
with altitude:

$$600 \quad n_{O_2} = n_{O_2,0} \cdot \exp(-z'/H) \quad (A1)$$

with the scale height  $H$ . In this case, the integral of eqEq. 3 directly yields  $H$ , i.e. the effective height equals the scale height  
for exponential profiles. For  $O_4$ , the profile is exponentially decreasing as well, with the scale height being half of that for  $O_2$ .  
Thus, for  $O_2$  profiles declining exponentially with  $z$ , the ratio of effective heights is just

$$\frac{h_{O_2}}{h_{O_4}} = 2. \quad (A2)$$

### 605 A2 Polytopic atmosphere

If the temperature is changing linearly with altitude, i.e. the dependence of  $T(z) = T_0 + \Gamma \cdot (z - z_0)$  is described by a constant  
lapse rate  $\Gamma$ , the resulting profile of  $O_2$  follows a power function:

$$n_{O_2} = n_{O_2,0} \cdot \left(1 + \frac{\Gamma}{T_0} z'\right)^{-\alpha}, \quad (A3)$$

with

$$610 \quad z' = z - z_0 \quad (A4)$$

being altitude above surface, and

$$\alpha = 1 + \frac{g \cdot M}{R \cdot \Gamma} \quad (A5)$$

being the constant exponent.

~~Integration of eq~~ Note that the for a constant lapse rate, temperature reaches 0 K at an altitude of

$$615 \quad \underline{\underline{z_{TOA} = \frac{T_0}{\Gamma}}} \quad (A6)$$

For  $T_0 = 300$  K and  $\Gamma = -6.5$  K km<sup>-1</sup>,  $z_{TOA}$  is about 46 km.

Thus, Eq. A3 is defined from  $z' = 0$  to  $z' = z_{TOA}$ , and  $n_{O_2}$  is set to 0 above.

Integration of Eq. 3 yields

$$\begin{aligned}
 h_{O_2} &= \int_0^{z_{TOA}} \left(1 + \frac{\Gamma}{T_0} z'\right)^{-\alpha} dz' \\
 &= \left[ \frac{1}{-\alpha + 1} \left(1 + \frac{\Gamma}{T_0} z'\right)^{-\alpha + 1} \cdot \frac{T_0}{\Gamma} \right]_0^{z_{TOA}} \\
 &= \frac{1}{-\alpha + 1} \cdot \frac{T_0}{\Gamma}
 \end{aligned} \tag{A7}$$

620 For  $O_4$ , the number density profile is

$$n_{O_4} = n_{O_4,0} \cdot \left(1 + \frac{\Gamma}{T_0} z'\right)^{-2\alpha}, \tag{A8}$$

~~and thus~~

and thus

$$h_{O_4} = \frac{1}{-2\alpha + 1} \cdot \frac{T_0}{\Gamma}. \tag{A9}$$

625 The ratio of effective heights can then be calculated as

$$\begin{aligned}
 \frac{h_{O_2}}{h_{O_4}} &= \frac{2\alpha - 1}{\alpha - 1} \\
 &= \frac{2 \frac{g \cdot M}{R \cdot \Gamma} + 1}{\frac{g \cdot M}{R \cdot \Gamma}} \\
 &= 2 + \frac{R}{g \cdot M} \cdot \Gamma.
 \end{aligned} \tag{A10}$$

For a lapse rate of 0 this equals the result for exponential profile (=2). For a typical lapse rate of ~~e.g. -6.5 K/km~~ -6.5 K km<sup>-1</sup>, the ratio of effective heights is 1.81.

~~Note that for solving the integral in eq. A7 analytically,~~

### 630 A3 Impact of the tropopause

In the previous section, the ratio of effective heights was calculated assuming a constant lapse rate ~~has to be assumed~~ throughout the atmosphere, ~~while in reality, the temperature profile is far more complex. For the calculation of the~~ A more realistic approach would be to assume a constant temperature above the tropopause (TP), as was done in Wagner et al. (2019). However, with the separation of the atmosphere in troposphere and stratosphere, it would not be possible to express the ratio of effective heights as simple function of the lapse rate as in Eq. A10. Thus, we decided to neglect the impact of the tropopause on the ratio of effective heights in the derivation of Eq. 10.

This causes a bias of  $V_{O_4, \Gamma}$  that can be easily quantified from Eq. 10 itself (applied at the tropopause instead of ground): The stratospheric  $O_4$  VCD, however, the troposphere ~~column~~ for constant  $T$  is  $\frac{C}{2} \cdot \frac{p_{TP}^2}{T_{TP}}$ , while it is  $\frac{C}{2 + \frac{R}{g \cdot M} \Gamma} \cdot \frac{p_{TP}^2}{T_{TP}}$  for constant

640 lapse rate. The difference is  $6 \cdot 10^{40}$  molecules<sup>2</sup> cm<sup>-5</sup> (for  $T_{TP} = 200$  K, where the assumption of a constant lapse rate is appropriate, contributes more than 95% of the total column. For the column above the tropopause, the assumption of a constant lapse rate causes an overestimation. In terms  $p_{TP} = 193$  hPa), which is about 0.45% of the total O<sub>4</sub>VCD, results based on eq. ?? are biased high by about 0.47% compared to the respective VCDs calculated by the method described in Wagner et al. (2019), assuming constant temperature above 12 km. This effect is quite small and thus neglected in eq. ?? For the empirical correction in 20, however, this effect is corrected implicitly. VCD.

#### 645 **A4 Real atmosphere**

For real atmospheric conditions, the lapse rate can generally not be considered to be constant. However, Thus, the O<sub>4</sub> VCD derived from Eq. 10 is higher than the respective VCD resulting from the profile construction proposed in Wagner et al. (2019). For  $V_{O_4, RH}$  (Eq. 14), this bias is eliminated by the empirical fit to the true O<sub>4</sub> VCD.

#### **A4 Side note: Determining the effective lapse rate from direct sun measurements of O<sub>2</sub> and O<sub>4</sub>**

650 The O<sub>4</sub> VCD depends on the ratio of effective heights can still be described by eq. ?? if an effective lapse rate is considered: for O<sub>2</sub> and O<sub>4</sub> (Eq. 6), which can be expressed by the atmospheric lapse rate (Eq. A10). This formalism might also be used in the other direction: from total column measurements of O<sub>2</sub> and O<sub>4</sub>, an effective atmospheric lapse rate can be derived.

$$2 + \frac{R}{g \cdot M} \cdot \Gamma_{\text{eff}} \stackrel{(A10)}{=} \frac{h_{O_2}}{h_{O_4}} \stackrel{-2}{=} \frac{(6)}{=} \frac{V_{O_2}}{V_{O_4}} \cdot \frac{g \cdot M}{R} n_{O_2,0} \stackrel{(8)}{=} \frac{V_{O_2}}{V_{O_4}} \cdot \frac{\nu_{O_2} \cdot p_0}{R \cdot T_0} \quad (A11)$$

and thus

$$655 \Gamma = \left( \frac{V_{O_2}}{V_{O_4}} \cdot \frac{\nu_{O_2} \cdot p_0}{R \cdot T_0} - 2 \right) \cdot \frac{g \cdot M}{R} \quad (A12)$$

This formalism might be applied to direct sun measurements, where light paths are well defined by the SZA. Even for limited accuracy of column measurements of O<sub>2</sub> and O<sub>4</sub>, this would allow to derive time series of an effective lapse rate, reflecting the state of the lower atmosphere.

## Appendix B: **WRF-model domains** Datasets

### 660 B1 Regional model and surface measurements

#### B1.1 WRF simulations

A nested domain centred at 49.12° N, 10.20° E was set up in Lambert conformal conic (LCC) projection with coarser domain (d01) at  $15 \times 15 \text{ km}^2$  horizontal resolution and finer domain (d02) at  $3 \times 3 \text{ km}^2$  resolution (Fig. B1). The spatial extent of the d01 domain is  $4800 \times 3416 \text{ km}^2$  while that for d02 is  $1578 \times 1473 \text{ km}^2$ . Vertically, the model extends from surface until 50 hPa with 42 terrain following layers in between. For constraining the meteorological initial and lateral boundary conditions, we use the ERA5 reanalysis dataset with a horizontal resolution of  $0.25^\circ \times 0.25^\circ$  and a temporal resolution of 3 hours, downloaded at pressure levels and at the surface. The soil classification, terrain height, and land use patterns were taken from the 21 category Noah-modified IGBP-MODIS land use data.

The model simulations were set up for May and June in 2018. The selection of data with  $\text{SZA} < 85^\circ$  results in a daily coverage from 6:00 h to 17:00 h UTC. Here we focus on model profiles in the d02 domain. The partial column of  $\text{O}_4$  above 50 hPa is considered accordingly in the calculation of the true  $\text{O}_4$  VCD (see Sect. 2.4).

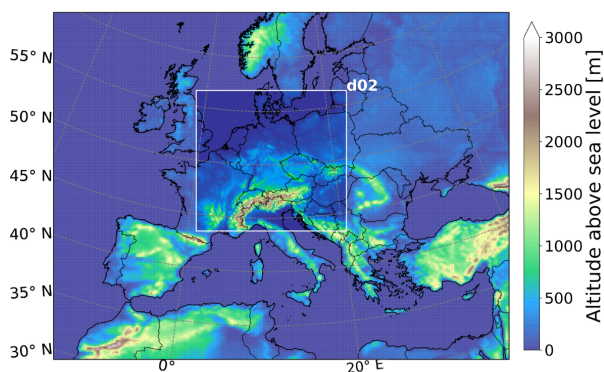


**Figure B1.** Nested model domains ~~used for~~ d01 (full figure) and d02 (marked pane) of the WRF simulations.

## Appendix C: **DWD stations**

### B0.1 DWD weather stations

Germany's National Meteorological Service (Deutscher Wetterdienst, DWD) provides hourly measurements of surface temperature, pressure and relative humidity for a network of ground stations in Germany (Kaspar et al., 2013). Data are provided via the climate data center web interface (CDC-v2.1; <https://cdc.dwd.de/portal/>). The meteorological measurements are performed in accordance to the guidelines of the world meteorological organization (WMO) to minimize local effects. Additionally,

we have applied quality control filters such that the parameters QUALITAETS\_BYTE (QB) is below 4 (thereby excluding untested, objected, and calculated values), and QUALITAETS\_NIVEAU (QN) is either 3 (automatic control and correction) or 7 (second control done, before correction) to only retain measurements of high quality. By applying these criteria, we retained 98.2 %, 100%, and 99.5% of  $T_0$ ,  $p_0$ , and  $RH_0$  data, respectively. Note that using only data with QN=10 (the best possible quality check level) would result in no data left for the period considered in this study. If only QN=7 had been applied, we would have retained the same number of  $T_0$  and  $RH_0$  but no  $p_0$  data.

For this study, we extract DWD measurements for May to June 2018, 6:00 to 17:00 UTC, and only consider stations providing  $T_0$ ,  $p_0$ , and  $RH_0$  simultaneously, resulting in 206 stations which are displayed in Fig. B1.

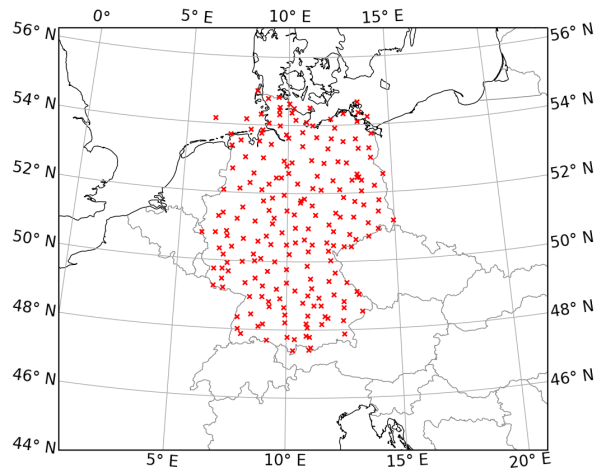


**Figure B1.** Location of the 206 DWD ground stations providing simultaneous measurements of surface values of  $T$ ,  $p$  and  $RH$  during ~~1-9~~ May to June 2018.

## Appendix C: ~~Validation of surface values from WRF~~

### B0.1 Validation of WRF surface values

We use the DWD network of surface stations for investigating the accuracy and precision of the WRF simulations. ~~Fig. ??~~ Figure B1 displays correlations between surface values from the DWD station network and the respective WRF simulations. For this purpose, each station is associated with the nearest neighbor from the WRF simulation. We do not interpolate the WRF data as we still want to compare the parameterized  $O_4$  VCD with the true VCD derived from vertical integration of the WRF profiles.

Surface altitude ( $a$ ) is lower in the gridded elevation map used as input in the WRF simulations by 20 m on average, and by almost 1 km for the station on Germany's highest mountain, Zugspitze. This is a consequence of the spatial resolution of the

695 WRF simulations of 1 km ~~net~~, which is not sufficient for resolving single mountains. The systematic negative bias of WRF surface altitude indicates that the DWD stations tend to be located on hill and mountain tops.

This difference in altitude would directly affect the comparisons of  $T$  and particularly  $p$ . Thus, we apply a simple correction of station values and extrapolate them to the respective WRF surface altitude assuming a lapse rate of  $-6.5 \text{ K km}^{-1}$ . For RH, no correction is applied.

700 ~~The reason for keeping the WRF values and adjusting the station data is that for WRF we have the full vertical profile and can calculate the true VCD according to eq. ??.~~

The comparison reveals a good agreement between surface values from WRF and DWD, with remaining systematic biases of WRF simulations of  $-1 \text{ K}$  for  $T_0$  and  $1 \%$  for  $\text{RH}_0$ .

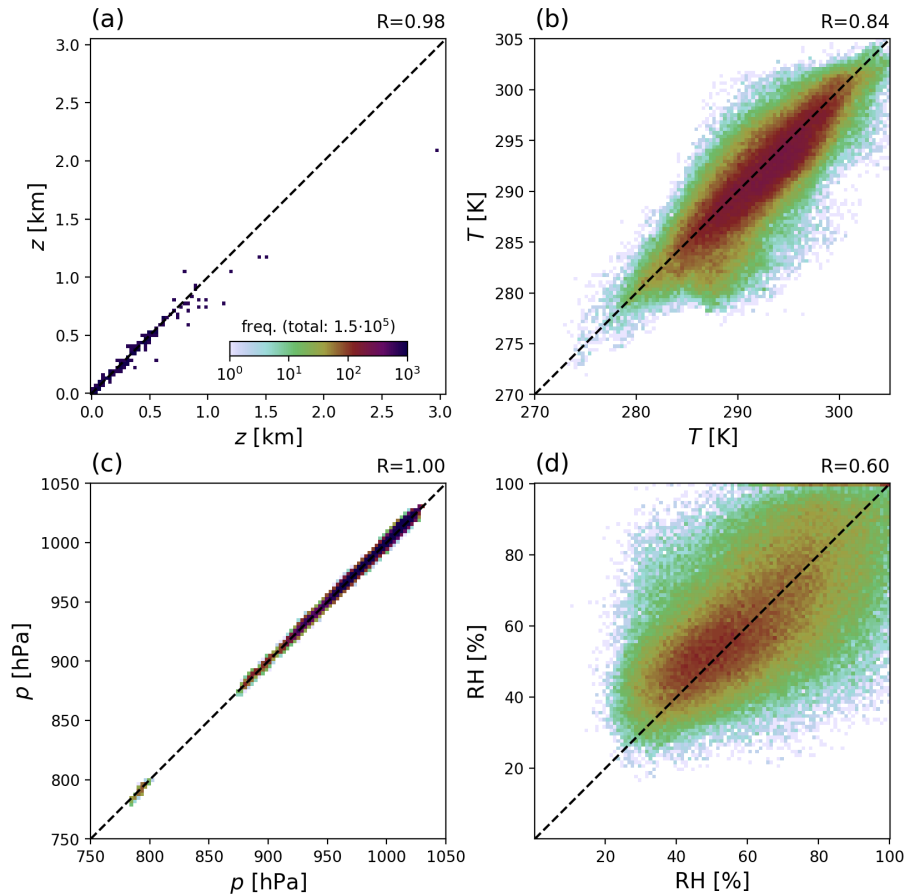


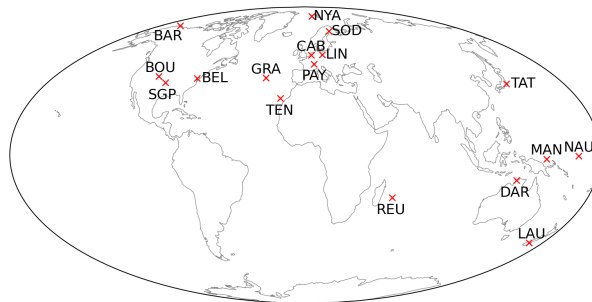
**Figure B1.** Comparison of WRF surface values (y axis) to DWD ground stations (x axis). For  $T$  and  $p$ , station values are adjusted to the mean altitude of the respective gridded elevation map used as input for WRF simulations (see text for details).

## Appendix C: GRUAN stations

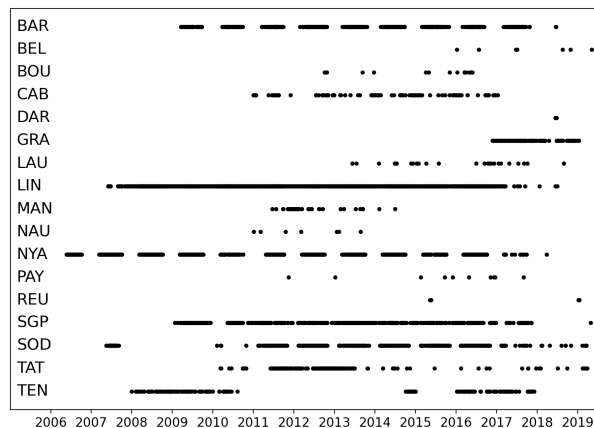
### 705 B1 GRUAN stations

Fig. ?? displays the location of the available GRUAN stations. Table B1 lists the stations, including their The GRUAN stations used in this study are listed in Table B1, including station shortcut and full name, and provides information on latitude, longitude, altitude of the station, and the number of available profiles with  $SZA < 85^\circ$ . Figure B1 displays a map showing the GRUAN station locations.

710 The temporal cover of radio sonde measurements at the different stations is displayed in Fig. B2. Note that some stations only contribute a low number of measurements. Still, we decided to keep all stations, as the application of a threshold for a minimum number of profiles of e.g. 50 would remove all tropical sites (Darwin, Manus and Nauru).



**Figure B1.** Location of GRUAN stations considered in this study. For station names and further details see [table Table B1](#).



**Figure B2.** Time of the available sonde flights (with  $SZA < 85^\circ$ ) for the GRUAN stations considered in this study. For station names and further details see [Table B1](#).

**Table B1.** List of GRUAN stations and number of available sonde flights (only considering  $\text{SZA} < 85^\circ$ ) used in this study.

Label	Name	Lat [ $^\circ$ N]	Lon [ $^\circ$ E]	$z_0$ [m]	Profiles
BAR	Barrow	71.32	-156.62	8	<del>1855</del> - <del>1189</del>
BEL	Beltsville	39.05	-76.88	53	<del>93</del> - <del>7</del>
BOU	Boulder	39.95	-105.20	1743	<del>128</del> - <del>13</del>
CAB	Cabauw	52.10	5.18	1	<del>381</del> - <del>98</del>
DAR	Darwin	-12.42	130.89	35	4
GRA	Graciosa	39.09	-28.03	30	<del>417</del> - <del>125</del>
LAU	Lauder	-45.05	169.68	371	<del>203</del> - <del>25</del>
LIN	Lindenberg	52.21	14.12	103	<del>4997</del> - <del>2255</del>
MAN	Manus	-2.06	147.43	4	<del>67</del> - <del>42</del>
NAU	Nauru	-0.52	166.92	7	<del>29</del> - <del>7</del>
NYA	NyAlesund	78.92	11.92	15	<del>1915</del> - <del>1059</del>
PAY	Payerne	46.81	6.95	491	<del>59</del> - <del>10</del>
REU	LaReunion	-21.08	55.38	2156	8
SGP	Lamont	36.61	-97.49	315	<del>3368</del> - <del>566</del>
SOD	Sodankyla	67.37	26.63	179	<del>1262</del> - <del>602</del>
TAT	Tateno	36.06	140.13	30	<del>589</del> - <del>165</del>
TEN	Tenerife	28.32	-16.38	121	<del>935</del> - <del>163</del>

## Appendix C: Additional ERA5 results

Figures C1 and C2 display additional results for  $\delta_{\Gamma}$  and  $\delta_{RH}$ , respectively, for 18 March, 18 September, and 18 December 2018.

715

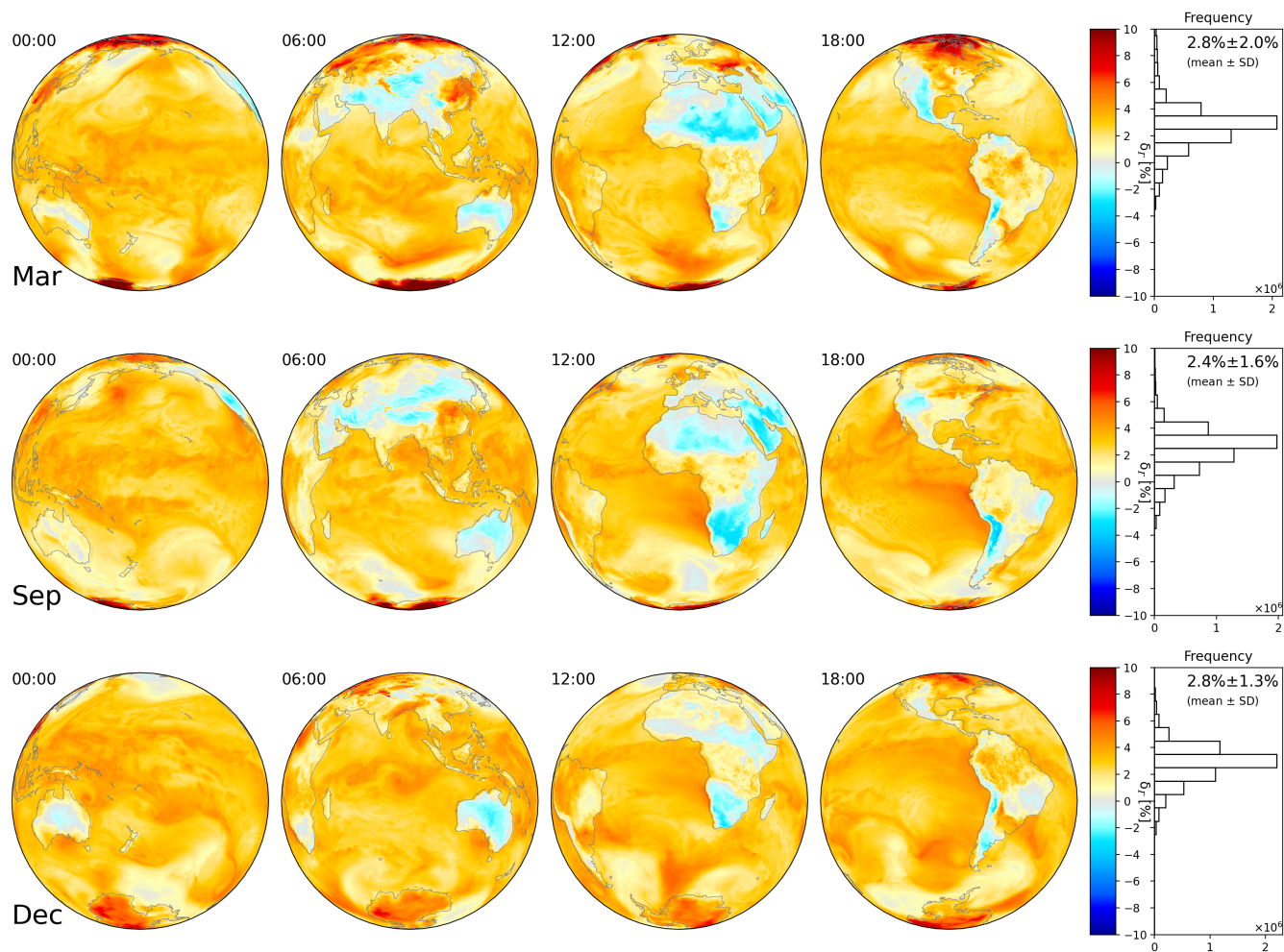


**Figure C1.** Deviation  $\delta_{\Gamma}$  according to Eq. 19 for ERA5 at 0:00, 6:00, 12:00 and 18:00 UTC on 18 March (top), 18 September (middle) and 18 December (bottom) 2018. The projection focuses on daytime for each timestep. On the right, the frequency distribution and mean and SD are given for all hourly outputs of the respective day.

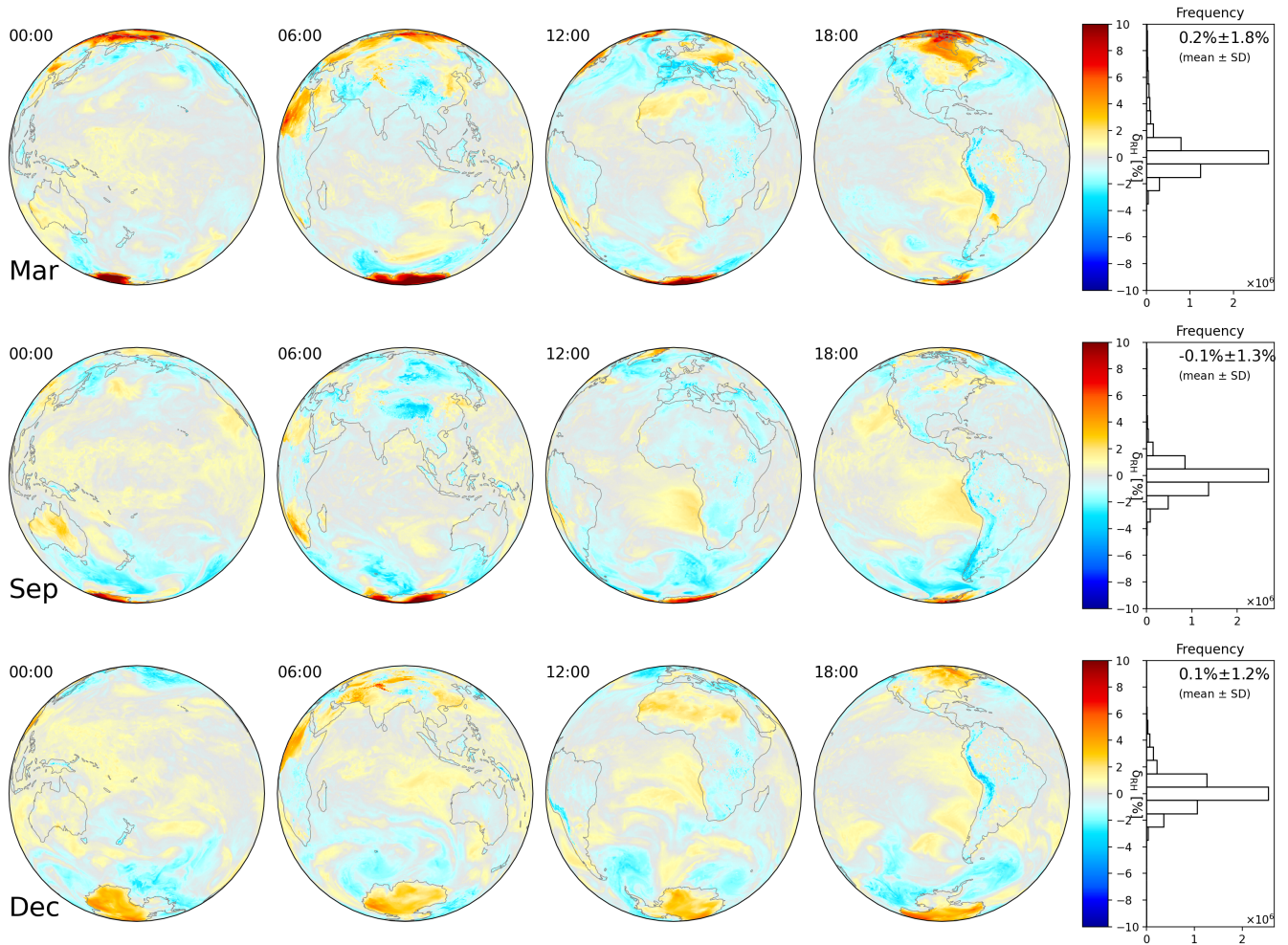


**Figure C2.** Deviation  $\delta_{RH}$  according to Eq. 19 for ERA5 at 0:00, 6:00, 12:00 and 18:00 UTC on 18 March (top), 18 September (middle) and 18 December (bottom) 2018. The projection focuses on daytime for each timestep. On the right, the frequency distribution and mean and SD are given for all hourly outputs of the respective day.

*Author contributions.* CB initiated this study by proposing to express the O<sub>4</sub> VCD by surface number density and column density of O<sub>2</sub>. VK performed the WRF simulations. SD processed ECMWF data. SD, CB and TW provided input on O<sub>4</sub> VCD calculation and meteorology. SB developed the full formalism, performed the intercomparisons to external datasets, and wrote the manuscript, with input and feedback from all co-authors.

720 *Competing interests.* None.

*Acknowledgements.* We would like to thank Rajesh Kumar (UCAR Boulder) and Sergey Osipov and Andrea Pozzer (both MPIC Mainz) for support in setting up the WRF simulations. We thank MPCDF Garching for providing computation resources for the WRF simulations. ERA Interim and ERA5 data used in this study are provided by the European Center of Medium-Range Weather Forecasts (ECMWF). Meteorological data for ground stations in Germany ~~was~~ were provided by Deutscher Wetterdienst (German Weather Service, DWD). Radiosonde  
725 measurements were provided by the GRUAN network.

## References

- Acarreta, J. R., de Haan, J. F., and Stammes, P.: Cloud pressure retrieval using the O<sub>2</sub>-O<sub>2</sub> absorption band at 477 nm, *J. Geophys. Res.*, 109, D05204, doi:10.1029/2003JD003915, 2004.
- 730 Beirle, S., Dörner, S., Donner, S., Remmers, J., Wang, Y., and Wagner, T.: The Mainz profile algorithm (MAPA), *Atmos. Meas. Tech.*, 12, 1785–1806, <https://doi.org/10.5194/amt-12-1785-2019>, 2019.
- Bodeker, G. E., Bojinski, S., Cimini, D., Dirksen, R. J., Haeffelin, M., Hannigan, J. W., Hurst, D. F., Leblanc, T., Madonna, F., Maturilli, M., Mikalsen, A. C., Philipona, R., Reale, T., Seidel, D. J., Tan, D. G. H., Thorne, P. W., Vömel, H. and Wang, J.: Reference Upper-Air Observations for Climate: From Concept to Reality, *Bulletin of the American Meteorological Society*, 97(1), 123–135, doi:10.1175/BAMS-D-14-00072.1, 2016.
- 735 Dirksen, R. J., Sommer, M., Immler, F. J., Hurst, D. F., Kivi, R., and Vömel, H.: Reference quality upper-air measurements: GRUAN data processing for the Vaisala RS92 radiosonde, *Atmos. Meas., Tech.*, 7, 4463–4490, <https://doi.org/10.5194/amt-7-4463-2014>, 2014.
- Greenblatt, G. D., Orlando, J., Burkholder, J. B., and Ravishankara, A. R.: Absorption measurements of oxygen between 330 and 1140 nm, *J. Geophys. Res.*, 95, 18577–18582, 1990.
- Heckel, A., Richter, A., Tarsu, T., Wittrock, F., Hak, C., Pundt, I., Junkermann, W., and Burrows, J. P.: MAX-DOAS measurements of formaldehyde in the Po-Valley, *Atmos. Chem. Phys.*, 5, 909–918, <https://doi.org/10.5194/acp-5-909-2005>, 2005.
- 740 Hersbach, H., Bell, B., Berrisford, P., Hirahara, S., Horányi, A., Muñoz-Sabater, J., Nicolas, J., Peubey, C., Radu, R., Schepers, D., Simmons, A., Soci, C., Abdalla, S., Abellan, X., Balsamo, G., Bechtold, P., Biavati, G., Bidlot, J., Bonavita, M., Chiara, G. D., Dahlgren, P., Dee, D., Diamantakis, M., Dragani, R., Flemming, J., Forbes, R., Fuentes, M., Geer, A., Haimberger, L., Healy, S., Hogan, R. J., Hólm, E., Janisková, M., Keeley, S., Laloyaux, P., Lopez, P., Lupu, C., Radnoti, G., Rosnay, P. de, Rozum, I., Vamborg, F., Villaume, S., and Thépaut, J.-N.: The ERA5 global reanalysis, *Q J R Meteorol Soc.*, 146, 1999–2049, <https://doi.org/10.1002/qj.3803>, 2020.
- 745 Kaspar, F., Müller-Westermeier, G., Penda, E., Mächel, H., Zimmermann, K., Kaiser-Weiss, A., and Deuschländer, T.: Monitoring of climate change in Germany – data, products and services of Germany’s National Climate Data Centre, in: *Advances in Science and Research, 12th EMS Annual Meeting and 9th European Conference on Applied Climatology (ECAC) 2012*, 99–106, <https://doi.org/10.5194/asr-10-99-2013>, 2013.
- 750 Kreher, K., Van Roozendaal, M., Hendrick, F., Apituley, A., Dimitropoulou, E., Frieß, U., Richter, A., Wagner, T., Lampel, J., Abuhassan, N., Ang, L., Anguas, M., Bais, A., Benavent, N., Bösch, T., Bogner, K., Borovski, A., Bruchkouski, I., Cede, A., Chan, K. L., Donner, S., Drosoglou, T., Fayt, C., Finkenzeller, H., Garcia-Nieto, D., Gielen, C., Gómez-Martín, L., Hao, N., Henzing, B., Herman, J. R., Hermans, C., Hoque, S., Irie, H., Jin, J., Johnston, P., Khayyam Butt, J., Khokhar, F., Koenig, T. K., Kuhn, J., Kumar, V., Liu, C., Ma, J., Merlaud, A., Mishra, A. K., Müller, M., Navarro-Comas, M., Ostendorf, M., Pazmino, A., Peters, E., Pinardi, G., Pinharanda, M., PETERS, A., Platt, U., Postlyakov, O., Prados-Roman, C., Puentedura, O., Querel, R., Saiz-Lopez, A., Schönhardt, A., Schreier, S. F., Seyler, A., Sinha, V., Spinei, E., Strong, K., Tack, F., Tian, X., Tiefengraber, M., Tirpitz, J.-L., van Gent, J., Volkamer, R., Vrekoussis, M., Wang, S., Wang, Z., Wenig, M., Wittrock, F., Xie, P. H., Xu, J., Yela, M., Zhang, C., and Zhao, X.: Intercomparison of NO<sub>2</sub>, O<sub>4</sub>, O<sub>3</sub> and HCHO slant column measurements by MAX-DOAS and zenith-sky UV–visible spectrometers during CINDI-2, *Atmos. Meas. Tech.*, 13, 2169–2208, <https://doi.org/10.5194/amt-13-2169-2020>, 2020.
- 760 Lawrence, M. G.: The Relationship between Relative Humidity and the Dewpoint Temperature in Moist Air: A Simple Conversion and Applications, *BAMS* 86, 225–234, <https://doi.org/10.1175/BAMS-86-2-225>, 2005.

- May, R. M., Arms, S. C., Marsh, P., Bruning, E., Leeman, J. R., Goebbert, K., Thielen, J. E., and Bruick, Z., 2021: MetPy: A Python Package for Meteorological Data. Unidata, <https://github.com/Unidata/MetPy>, doi:10.5065/D6WW7G29.
- Platt, U. and Stutz, J.: Differential Optical Absorption Spectroscopy, Springer-Verlag Berlin Heidelberg, 2008.
- 765 Romps, D. M.: Exact Expression for the Lifting Condensation Level, *J. Atmos. Sci.* 74, 3891–3900, <https://doi.org/10.1175/JAS-D-17-0102.1>, 2017.
- Skamarock, W. C., Klemp, J. B., Dudhia, J., Gill, D. O., Liu, Z., Berner, J., Wang, W., Powers, J. G., Duda, M. G., Barker, D. M., and Huang, X.-Y.: A Description of the Advanced Research WRF Model Version 4, UCAR/NCAR, <https://doi.org/10.5065/1DFH-6P97>, 2019.
- Sommer, M., Dirksen, R., and Immler, F.: RS92 GRUAN Data Product Version 2 (RS92-GDP.2), GRUAN Lead Centre, DOI:10.5676/GRUAN/RS92-GDP.2, 2012.
- 770 Thalman, R. and Volkamer, R.: Temperature dependent absorption cross-sections of O<sub>2</sub>–O<sub>2</sub> collision pairs between 340 and 630 nm and at atmospherically relevant pressure, *Phys. Chem. Chem. Phys.*, 15(37), 15371–15381, doi:10.1039/C3CP50968K, 2013.
- Tohjima, Y., Machida, T., Watai, T., Akama, I., Amari, T., and Moriwaki, Y.: Preparation of gravimetric standards for measurements of atmospheric oxygen and reevaluation of atmospheric oxygen concentration, *JGR 110 (D11)*, <https://doi.org/10.1029/2004JD005595>, 2005.
- 775 Veefkind, J. P., de Haan, J. F., Sneep, M., and Levelt, P. F.: Improvements to the OMI O<sub>2</sub>–O<sub>2</sub> operational cloud algorithm and comparisons with ground-based radar–lidar observations, *Atmos. Meas. Tech.*, 9, 6035–6049, <https://doi.org/10.5194/amt-9-6035-2016>, 2016.
- Wagner, T., Erle, F., Marquard, L., Otten, C., Pfeilsticker, K., Senne, T., Stutz, J., and Platt, U.: Cloudy sky optical paths as derived from differential optical absorption spectroscopy observations, *JGR 103*, 25307–25321, <https://doi.org/10.1029/98JD01021>, 1998.
- Wagner, T., Beirle, S., Benavent, N., Bösch, T., Chan, K. L., Donner, S., Dörner, S., Fayt, C., Frieß, U., García-Nieto, D., Gielen, C., 780 González-Bartolome, D., Gomez, L., Hendrick, F., Henzing, B., Jin, J. L., Lampel, J., Ma, J., Mies, K., Navarro, M., Peters, E., Pinardi, G., Puentedura, O., Pukite, J., Remmers, J., Richter, A., Saiz-Lopez, A., Shaiganfar, R., Sihler, H., Van Roozendaal, M., Wang, Y., and Yela, M.: Is a scaling factor required to obtain closure between measured and modelled atmospheric O<sub>4</sub> absorptions? An assessment of uncertainties of measurements and radiative transfer simulations for 2 selected days during the MAD-CAT campaign, *Atmos. Meas. Tech.*, 12, 2745–2817, <https://doi.org/10.5194/amt-12-2745-2019>, 2019.
- 785 Wagner, T., Dörner, S., Beirle, S., Donner, S., and Kinne, S.: Quantitative comparison of measured and simulated O<sub>4</sub> absorptions for one day with extremely low aerosol load over the tropical Atlantic, *Atmos. Meas. Tech.*, 14, 3871–3893, <https://doi.org/10.5194/amt-14-3871-2021>, 2021.
- World Meteorological Organization (WMO): Guide to Instruments and Methods of Observation, Volume I: Measurement of Meteorological Variables, 2018 Edition, WMO, Geneva, ISBN 978-92-63-10008-5, online available at [https://library.wmo.int/index.php?lvl=notice\\_](https://library.wmo.int/index.php?lvl=notice_display&id=12407#.YO1QPEyxXYQ)  
790 [display&id=12407#.YO1QPEyxXYQ](https://library.wmo.int/index.php?lvl=notice_display&id=12407#.YO1QPEyxXYQ), last access 13 July 2021, 2018.